J. Fluid Mech. (1978), *vol.* 89, *part* 2, *pp.* 305–342
Printed in Great Britain

Similarity treatment of moving-equilibrium turbulent boundary layers in adverse pressure gradients

By B. A. KADER

Moscow Institute of Mechanical Engineering for Chemical Industry, K. Marx St. 21/4, Moscow

AND A. M. YAGLOM

Institute of Atmospheric Physics, Academy of Sciences of USSR, Pyzhevsky 3, Moscow

(Received 27 October 1977 and in revised form 17 March 1978)

Dimensional analysis is applied to the velocity profile $U(y)$ of turbulent boundary layers subjected to adverse pressure gradients. It is assumed that the boundary layer is in moving or local equilibrium in the sense that the free-stream velocity U_∞ and kinematic pressure gradient $\alpha = \rho^{-1}dP/dx$ vary only slowly with the co-ordinate x. This assumption implies a rather complicated general equation for the velocity gradient dU/dy which may be considerably simplified for several specific regions of the flow. A general family of velocity profiles is derived from the simplified equations supplemented by some experimental information. This family agrees well with almost all existing data on velocity profiles in adverse-pressure-gradient turbulent boundary layers. It may be used for the derivation of a skin-friction law which predicts satisfactorily the values of the wall shear stress at any non-negative value of the pressure gradient. The variation of the boundary-layer thickness with x is also predicted by dimensional considerations.

1. Introduction

Turbulent boundary layers with longitudinal pressure gradients are flows of great significance for many engineering problems. Therefore it is not at all surprising that an enormous literature is devoted to the study of such layers (only a small part of it is cited in this paper). The basic reference on the subject is the two-volume *Proceedings of the* 1968 *AFOSR–IFP Stanford Conference* (Kline *et al.* 1969; Coles & Hirst 1969). Volume 1 of these Proceedings is devoted to various methods of computation of turbulent boundary layers, while volume 2 contains a collection of experimental data that were recommended for verification of future theories on boundary layers with pressure gradients. This recommendation shows that none of the theories discussed at the Stanford Conference was considered to be fully satisfactory and hence to make further theoretical development redundant. In fact several monographs and many tens, if not hundreds, of theoretical papers on boundary layers with pressure gradients were published after the Stanford Conference; typical examples are the monographs by Fedyaevskii, Ginevskii & Kolesnikov (1973) and Cebeci & Smith (1974) or the papers by Allan & Sharma (1974), Reeves (1974), Lapin & Sharov (1974), Kreskovsky, Shamroth & McDonald (1975), Head (1976), Novozhilov (1976), and Ng & Spalding (1976). Nevertheless, so far there is no theory on general turbulent boundary layers with pressure gradients which is generally accepted as sufficiently accurate.

All the theoretical approaches in the book edited by Kline *et al.* (1969) and in all the subsequent work are based on certain hypotheses, e.g. closing hypotheses applied to close the Reynolds equations for the mean velocity field or a system of dynamical equations for the mean velocity and some of the higher-order moments of flow variables. However, none of the closing hypotheses nor any of the other proposed hypotheses is rigorous, and the physical basis of all of them is of limited soundness. Therefore it seems reasonable to try another way and to study the laws of turbulent boundary layers implied by general dimensional and similarity arguments alone without any use of dynamic equations and specific hypotheses. Of course, it should not be expected that these arguments alone will yield a complete solution of the problem. However, it is known that combination of dimensional arguments with some additional physical arguments and a few relations extracted from experimental information often permits one to find satisfactory solutions for various applications [cf., for example, the Monin–Oboukhov similarity theory of surface-layer atmospheric turbulence expounded in Monin & Yaglom (1971, chap. 4) or the derivation of heat and mass transfer laws for turbulent wall flows proposed by Kader & Yaglom (1972, 1977*a*) and Yaglom & Kader (1974)]. It will be shown below that a similar approach may also be rather successfully applied to a wide variety of turbulent boundary layers in adverse pressure gradients.

Let us now describe the class of turbulent boundary layers studied in the present paper. We shall consider only two-dimensional steady turbulent flows in the x direction along a flat impermeable wall coinciding with the plane $y = 0$. Unless stated otherwise, the wall will be assumed to be smooth and the pressure gradient to be positive. Moreover one more requirement will be introduced which is basic for the use of similarity and dimensional arguments. Namely, we shall assume that the boundary layer is in moving equilibrium in the following sense: the free-stream velocity U_∞ and kinematic pressure gradient $\alpha = \rho^{-1}dP/dx$ vary only slowly with the co-ordinate x so that the boundary layer adjusts to these variations and its structure at any value of x depends essentially on the relevant local parameters (at the same x) only and not on the upstream history of the flow. The assumption of a moving equilibrium may seem to be rather restrictive since it excludes the appearance of the so-called historical region within the flow and such a region is mentioned in some important studies (see, for example, Perry, Bell & Joubert 1966). However, in fact the class of boundary layers that can be considered to be in moving equilibrium is very wide and includes many important types of flows. It is easily seen, for example, that all the 'equilibrium boundary layers' of Clauser (1956) are in moving equilibrium, as well as the related near-equilibrium (pseudo-equilibrium) turbulent boundary layers of Head (1976). A moving-equilibrium condition will be also satisfied by all the gradually developing 'self-preserving' turbulent boundary layers of Townsend (1965, 1976, chap. 7). Let us also note that models of turbulent boundary layers evidently satisfy the moving-equilibrium condition if they may be represented by velocity-profile families which include only the local values of flow parameters (at a given value of x) and no upstream values (e.g. the wall-and-wake profiles of Coles; see Coles & Hirst 1969, pp. 1–45; Monin & Yaglom 1971, §5.6; or Allan & Sharma 1974). The same condition is satisfied for many semi-empirical theories of turbulent boundary layers which are based on model dynamical equations which include no upstream values of flow parameters (see, for example, Kline *et al.* 1969; Fedyaevskii *et al.* 1973). The

investigation of the general conditions guaranteeing the moving-equilibrium character of the boundary layer is beyond the scope of this paper, although some related remarks will be given at the end of the next section. At present we just note that the subsequent results will also show the possibility of satisfactory description of a wide collection of adverse-pressure-gradient boundary-layer data by the equations which do not violate the moving-equilibrium condition. Also some indications of the comparatively small deviations of the boundary layers considered from moving equilibrium will be given below.

A preliminary report on this study was published as a short note by Kader & Yaglom (1977*b*). The main results of this note are included in a refined and partially modified form in the present paper.

2. Similarity laws for turbulent boundary layers in moving equilibrium

Let us consider the vertical velocity profile $U = U(y)$ at a given cross-section $x =$ constant of a turbulent boundary layer in moving equilibrium. This profile may depend on the physical properties of the fluid and the local values (at the given x) of external physical parameters affecting the flow. We shall consider only kinematic parameters that are independent of the unit of mass. Then the kinematic molecular viscosity ν will be the only necessary physical property of the fluid and the set of necessary external parameters will include the free-stream velocity U_∞, the boundary-layer thickness δ (determined by the condition $U(\delta) = 0{\cdot}99U_\infty$) and the kinematic pressure gradient $\alpha = \rho^{-1}dP/dx$.† It is often convenient to use the friction velocity $u_* = (\tau_w/\rho)^{\frac{1}{2}}$, where τ_w is the wall shear stress, instead of the free-stream velocity U_∞; this replacement will be widely used below. It is without any importance since the analysis must also give us a skin-friction law which permits us to determine the ratio u_*/U_∞ (or equivalently the skin-friction coefficient $c_f = 2(u_*/U_\infty)^2$) as a function of ν, U_∞, δ and α.

Only the case of positive values of α will be analysed in detail in this paper; however at first we assume that α may have any sign (i.e. both adverse and favourable pressure gradients will be considered). Three independent length scales can be formulated from the four quantities ν, u_*, δ and α. They are the viscous length scale $\delta_v = \nu/u_*$, the pressure-gradient length scale $\delta_p = u_*^2/|\alpha|$ and the external length scale δ. We shall consider only the case of a fully developed turbulent flow where the Reynolds number

$$Re = U_\infty \delta/\nu$$

is very high and therefore $Re_* = u_* \delta/\nu = Re\,(\frac{1}{2}c_f)^{\frac{1}{2}}$ is much greater than one, i.e. $\delta \gg \delta_v$. As a rule (though not always) we shall also suppose that $|\alpha|$ is large enough to provide the inequality $u_*^2/|\alpha| = \delta_p \ll \delta$ but small enough to provide the inequality $\delta_p \gg \delta_v = \nu/u_*$. In this case we shall have three very different length scales

$$\delta_v \ll \delta_p \ll \delta,$$

† It is also possible to assume that the derivatives $\alpha'(x) = d\alpha/dx$, $\alpha''(x)$, ... of the function $\alpha(x)$ influence, to a certain extent, the velocity profile $U(y)$ (see, for example, Perry 1966, whose conclusions were disputed by McDonald 1969). However, the assumption of a moving equilibrium presupposes implicitly that $\alpha(x)$ varies only slowly with x. Therefore it seems reasonable at first to neglect the influence of the derivatives of $\alpha(x)$ with respect to x. It will be shown below that such an approximate analysis leads to quite satisfactory results. That is why a more general assumption will not be considered in the present paper.

which implies that the whole flow field can be divided into several regions described by different similarity laws.

In fact, the distribution of the velocity gradient dU/dy in the flow considered can be described by a function of three dimensionless arguments according to the well-known π-theorem of dimensional analysis (see Bridgman 1932, chap. 4). The corresponding description can be presented in several different forms; in particular, it can be written as any of the following three equivalent equations:

$$\frac{dU}{dy} = \frac{u_*}{y}\phi_1\left(\frac{yu_*}{\nu}, \quad \frac{u_*^3}{|\alpha|\nu}, \quad \frac{\delta u_*}{\nu}\right) \tag{1a}$$

$$= \frac{|\alpha|^{\frac{1}{2}}}{y^{\frac{1}{2}}}\phi_2\left(\frac{y|\alpha|}{u_*^2}, \quad \frac{\delta|\alpha|}{u_*^2}, \quad \frac{\delta u_*}{\nu}\right) \tag{1b}$$

$$= \frac{|\alpha|^{\frac{1}{2}}}{\delta^{\frac{1}{2}}}\phi_3\left(\frac{y}{\delta}, \quad \frac{\delta|\alpha|}{u_*^2}, \quad \frac{\delta u_*}{\nu}\right). \tag{1c}$$

Here $\phi_1(y+, r, Re_*)$, $\phi_2(\zeta, s, Re_*)$ and $\phi_3(\eta, s, Re_*)$ are three universal functions which can be easily expressed in terms of one another. (These functions may clearly have different forms for $\alpha \gtrless 0$.)

If $y \ll \delta_p = u_*^2/|\alpha|$ (and hence *a fortiori* $y \ll \delta$), then the length scales δ_p and δ will not affect the flow significantly. Therefore it is convenient to use here (1*a*), where the arguments $r = \delta_p/\delta_v$ and $Re_* = \delta/\delta_v$ are replaced by infinity. It is natural to suppose (although this supposition cannot be proved rigorously) that there exists a bounded limit

$$\phi_1(y+) = \phi_1(y+, \infty, \infty) = \lim_{r\to\infty \;\; Re_*\to\infty} \phi_1(y+, r, Re_*).$$

This implies the existence of the usual Prandtl wall law for $y \ll \delta_p$:

$$\frac{dU}{dy} = \frac{u_*}{y}\phi_1\left(\frac{yu_*}{\nu}\right). \tag{2}$$

We see that the wall law must have the usual form in flows with pressure gradients if $\delta_p \gg \delta_v$, $y \ll \delta_p$ and $y \ll \delta$. However, if $r = \delta_p/\delta_v$ is not great enough (but $Re_* = \delta/\delta_v \gg 1$), then

$$\frac{dU}{dy} = \frac{u_*}{y}\phi_1\left(\frac{yu_*}{\nu}, \quad \frac{u_*^3}{|\alpha|\nu}\right), \tag{2a}$$

where $\phi_1(y+, r) = \phi_1(y+, r, \infty)$ is a universal function of two variables.

In the region $y \gg \delta_v = \nu/u_*$ the eddy viscosity is of order $u_* y$ and is much greater than the molecular viscosity ν. Hence the influence of the molecular viscosity on the vertical momentum transfer can be neglected in this region. This remark implies that, when $\delta \gg \delta_v$ (i.e. $Re_* \gg 1$), the so-called *Reynolds number similarity* must be valid at $y \gg \delta_v$. The Reynolds number similarity principle asserts that all the flow parameters are independent of the molecular viscosity and hence also the Reynolds numbers Re and Re_* (see Townsend 1976, § 5.7). This principle implies that the function $\phi_1(yu_*/\nu)$ on the right-hand side of (2) may be replaced by a constant $\phi_1(\infty) = A$ when $y \gg \nu/u_*$. This replacement leads us to the well-known equations of the logarithmic layer:

$$dU/dy = Au_*/y, \quad U(y) = u_*[A \ln(yu_*/\nu) + B]. \tag{3}$$

Let us also note that in case of a homogeneous rough wall with protrusions of mean height h the function $\phi_1(yu_*/\nu)$ in (2) must be replaced by a more complicated function

$\phi_1(yu_*/\nu,\ hu_*/\nu,\ \sigma_1,\ \sigma_2,\ \ldots)$, where $\sigma_1,\ \sigma_2,\ \ldots$ are dimensionless parameters which characterize the shapes and spatial distribution of the roughness elements. The functions $\phi_1(yu_*/\nu)$ and $\phi_1(yu_*/\nu,\ hu_*/\nu,\ \sigma_1,\ \sigma_2,\ \ldots)$ approach the same limit A as $yu_*/\nu \to \infty$, but the velocity profile within the logarithmic layer above a rough wall (i.e. at $y \gg \nu/u_*$ and $y \gg h$) is given by the modified equation

$$U(y) = u_*[A \ln (yu_*/\nu) + B - B'], \quad B' = B'(hu_*/\nu, \sigma_1, \sigma_2, \ldots) \tag{3a}$$

(cf. Monin & Yaglom 1971, § 5.4; Hinze 1975, § 7.5; Townsend 1976, § 5.5). It follows from this that the rough-wall velocity profile within the logarithmic layer and above it may be obtained from the corresponding smooth-wall velocity profile at the same values of u_*, ν, α and δ by the subtraction of a constant velocity B' from all the values $U(y)$. A similar situation occurs in the case of turbulent flow along a smooth wall of dilute solutions of drag-reducing polymers. The only difference is that here all the velocity values $U(y)$ within the logarithmic layer increase by a constant amount in comparison with the corresponding values in ordinary fluid flow. Hence in such a case the velocity profile is also given by (3*a*) but the quantity B' is negative. (B' depends here on ν, u_* and the polymer concentration and type; cf. Huang 1974, where many additional references can be found.) Therefore, if the influence of the pressure gradient does not eliminate the logarithmic layer, then the cases of rough-wall flow and flow of a dilute polymer solution do not need special consideration. So neither of these cases will be mentioned below.

The conditions $\delta_v \ll y \ll \delta$ must determine a special 'gradient layer' characterized by the property that here the molecular viscosity and the length scales δ_v and δ do not affect the flow significantly. It is convenient to use (1*b*) within this layer and to replace large arguments $s = \delta|\alpha|/u_*^2 = \delta/\delta_p$ and $Re_* = \delta/\delta_v$ by infinity on the right-hand side of (1*b*). If we assume that a finite limit $\phi_2(\zeta, \infty, \infty) = \phi_2(\zeta)$ exists, then we obtain the following equation:

$$\frac{dU}{dy} = \frac{|\alpha|^{\frac{1}{2}}}{y^{\frac{1}{2}}} \phi_2\left(\frac{y|\alpha|}{u_*^2}\right). \tag{4}$$

However, if in a fully developed turbulent flow (i.e. at $Re_* \gg 1$) the value of

$$\delta/\delta_p = \delta|\alpha|/u_*^2 = s$$

is not large enough, then the argument $\delta|\alpha|/u_*^2$ of ϕ_2 must be preserved in (1*b*). Hence in this case the equation

$$\frac{dU}{dy} = \frac{|\alpha|^{\frac{1}{2}}}{y^{\frac{1}{2}}} \phi_2\left(\frac{y|\alpha|}{u_*^2}, \frac{\delta|\alpha|}{u_*^2}\right) \tag{4a}$$

will be valid at $y \gg \delta_v$.

Later we shall consider only the case of decelerating flows with $\alpha > 0$. In such a case the flow region determined by the condition $y \gg \delta_p = u_*^2/\alpha$ deserves a special study. The fluid-dynamic equations imply that the relation $d\tau/dy = dP/dx = \rho\alpha$, where $\tau = \rho\nu\, dU/dy - \rho\overline{u'v'}$ is the total stress, is valid at the wall (i.e. when $y = 0$) in a two-dimensional steady flow along a smooth wall (see, for example, Monin & Yaglom 1971, § 5.2; or Townsend 1976, § 5.2). Therefore

$$\tau(y) = \tau_w + \rho\alpha y + \ldots \tag{5}$$

in the vicinity of the wall if $\alpha > 0$. The form given by (5) is not very accurate because mean-flow inertia has been neglected (McDonald 1969; Townsend 1976, § 5.15);

nevertheless this equation can be used for the estimation of the order of the magnitude of the shear stress variation for a two-dimensional boundary layer in an adverse pressure gradient. From (5) it can be seen that the increase in the shear stress from $y = 0$ to a given y exceeds $\tau_w = \rho u_*^2$ significantly, if $\alpha > 0$ and $y \gg \delta_p = u_*^2/\alpha$. Hence the value of a shear stress for $y \gg \delta_p$ depends on the wall stress τ_w only slightly, and is determined mainly by other factors. It seems natural to suppose that when $\alpha > 0$ and $y \gg \delta_p$ *a wall stress similarity principle* is valid according to which the value of $u_* = (\tau_w/\rho)^{\frac{1}{2}}$ can be excluded here from the list of physical quantities which affect the flow significantly. The application of this principle to (4) leads to the conclusion that the function $\phi_2(y\alpha/u_*^2) = \phi_2(y/\delta_p)$ must be close to the constant $\phi_2(\infty) = \frac{1}{2}\mathscr{K}$ when $\alpha > 0$ and $y \gg \delta_p$. Hence the so-called 'half-power law' must be valid for the velocity profile in the region $\delta_p \ll y \ll \delta$; according to this law

$$dU/dy = \tfrac{1}{2}\mathscr{K}(\alpha/y)^{\frac{1}{2}}, \quad U(y) = \mathscr{K}(\alpha y)^{\frac{1}{2}} + \mathscr{K}_1. \tag{6}$$

Another derivation of the 'half-power law' will be given later in this section.

If y is of the order of δ, then the velocity profile is most conveniently described by (1*c*). When $Re_* \gg 1$ and, in addition, $\alpha > 0$ and $y \gg \delta_p$, Reynolds number similarity and wall stress similarity will be valid simultaneously. This implies that the last two arguments of the function $\phi_3(\eta, s, Re_*)$ can be replaced by the infinity and hence

$$\frac{dU}{dy} = \left(\frac{\alpha}{\delta}\right)^{\frac{1}{2}} \phi_3\left(\frac{y}{\delta}\right), \quad \frac{U_\infty - U(y)}{(\alpha\delta)^{\frac{1}{2}}} = \Phi_3\left(\frac{y}{\delta}\right), \tag{7}$$

where $\phi_3(\eta) = \phi_3(\eta, \infty, \infty)$ and

$$\Phi_3(\eta) = \int_2^1 \phi_3(\eta')\, d\eta'.$$

If, however, $\alpha < 0$ or the ratio δ/δ_p is not great enough, then the wall stress similarity principle will be inapplicable. Therefore the argument $s = \delta/\delta_p$ of the function ϕ_3 must be retained here and (7) take the form

$$\frac{dU}{dy} = \left(\frac{|\alpha|}{\delta}\right)^{\frac{1}{2}} \phi_3\left(\frac{y}{\delta}, \frac{|\alpha|\delta}{u_*^2}\right), \quad \frac{U_\infty - U(y)}{(|\alpha|\delta)^{\frac{1}{2}}} = \Phi_3\left(\frac{y}{\delta}, \frac{|\alpha|\delta}{u_*^2}\right). \tag{7a}$$

Let us now assume that the boundary layer includes both the 'gradient layer' and the 'velocity defect layer' and also that the maximum value of y for which the gradient law (4) is valid is greater than the minimum value of y for which the velocity defect law (7) is valid. Then an overlap layer exists where the laws (4) and (7) are valid simultaneously. In such a layer the following equalities will be satisfied:

$$\left(\frac{y}{\alpha}\right)^{\frac{1}{2}} \frac{dU}{dy} = \phi_2\left(\frac{y\alpha}{u_*^2}\right) = \left(\frac{y}{\delta}\right)^{\frac{1}{2}} \phi_3\left(\frac{y}{\delta}\right).$$

Hence here

$$\phi_2\left(\frac{y\alpha}{u_*^2}\right) = \left(\frac{y}{\delta}\right)^{\frac{1}{2}} \phi_3\left(\frac{y}{\delta}\right) = \tfrac{1}{2}\mathscr{K}, \tag{8}$$

where $\mathscr{K}$ = constant. Substitution of equation (8) for ϕ_2 into (4) leads again to the 'half-power law'; this is the second derivation of this law mentioned above. Moreover substitution of equation (8) for ϕ_3 in the first of equations (7) yields

$$[U_\infty - U(y)]/(\alpha\delta)^{\frac{1}{2}} = -\mathscr{K}(y/\delta)^{\frac{1}{2}} + I, \tag{9}$$

where I is an integration constant. The order of the magnitude of I may be roughly

estimated by the assumption that (9) is valid till the outer edge of the boundary layer. In fact the left-hand side of (9) must vanish at $y = \delta$ and hence the stated assumption implies that $I \approx \mathscr{K}$. However, this assumption is not strictly valid and therefore the implied estimate of I cannot be expected to be precise.

Only boundary layers along a flat plate have been considered in the above discussion. It is clear, however that all the equations considered can also be applied to the flows in channels with parallel walls, in straight circular tubes (where the y axis is perpendicular to the tube wall) and in plane or axially symmetric diffusers or contractions if the boundary-layer thickness δ is smaller than a typical vertical flow length scale $\mathscr{D}$ (the half-width for plane flows and the radius for axially symmetric flows). The situation is slightly more complicated when boundary layers along opposite walls merge with each other and fill the whole flow region (for example, in steady developed turbulent flows in a channel, tube, diffuser or contraction). Here the vertical flow length scale $\mathscr{D}$ plays the role of the length scale δ. It is natural to assume that all the above-mentioned equations which do not contain δ (i.e. are independent of the flow conditions at y values of the order of δ) will be also applicable to such flows, while the equations containing δ will be applicable only when δ is replaced by $\mathscr{D}$, in which case the functions in these equations may have different forms for different types of flow. However, we shall not consider the cases of merging opposite boundary layers in the present paper. (Let us also note that α is always negative in channel, tube and contraction flows.)

The considerations mentioned above may be used for the derivation of some conditions which are apparently necessary for the flow to be in moving equilibrium. In fact, it has already been explained that only two dimensional parameters α and δ affect significantly the flow in the outer region of a boundary layer if $Re_* \gg 1$, $\alpha > 0$ and $\delta \gg \delta_p$. Therefore the typical time scale ('relaxation time scale') in this region is proportional to $T_0 = (\delta/\alpha)^{\frac{1}{2}}$. Furthermore, the typical time scale of the longitudinal variations in the free-stream velocity U_∞ is equal to $|dU_\infty/dx|^{-1} = U_\infty/\alpha$. These longitudinal variations are the main reason for the change in the boundary-layer conditions along the x axis; hence it is natural to suppose that a boundary layer with $\alpha > 0$ and $\delta \gg \delta_p$ can be in moving equilibrium only when $(\delta/\alpha)^{\frac{1}{2}} \ll U_\infty/\alpha$, i.e.

$$U_\infty/(\alpha\delta)^{\frac{1}{2}} \gg 1.$$

It will be seen from the data analysed in the present paper that in fact the value of $U_\infty/(\alpha\delta)^{\frac{1}{2}}$ need not be very great to guarantee a moving equilibrium. However a moving equilibrium is only approximately valid when the value of the above-mentioned ratio is considerably smaller than ten (see figure 11 and the corresponding discussion in the text). We also mention that the above condition is only necessary and not sufficient for moving equilibrium. It is natural to expect, for example, that longitudinal variations of the kinematic pressure gradient $\alpha(x)$ do not influence the flow if

$$\left(\frac{U_\infty}{\alpha}\frac{d\alpha}{dx}\right)^{-1} \gg \left(\frac{\delta}{\alpha}\right)^{\frac{1}{2}}, \quad \text{i.e. } \alpha^{\frac{3}{2}}/U_\infty \delta^{\frac{1}{2}}\alpha' \gg 1.$$

Moreover, moving equilibrium will not occur for separation and near-separation flows; therefore such flows will not usually be considered in the present paper.

Many of the above-mentioned similarity laws are well known and can be found in some form in the enormous literature on turbulent wall flows. A number of the related

references will be given in the next section of the paper. However, we do not know of any sources where all these similarity laws are considered simultaneously. Moreover, the similarity laws are usually supplemented by some quite different assumptions of varying degrees of soundness while we tend to avoid all such assumptions in the present paper. Below we restrict ourselves deliberately to determination of all the functions and constants of the similarity theory by a pure treatment of the existing experimental data. This does not mean, of course, that we consider dynamic equations to be useless for the study of turbulent boundary layers. We are sure that the dynamic theory and intelligently selected closure hypotheses can be quite helpful for the refined determination of the similarity functions and constants, the control of the physical realizability of the results and the detailed study of the limits of the applicability of the assumption of moving equilibrium. However, all the deductions from the dynamic theory must first of all be compared with the existing data, and use of the general similarity equations may considerably facilitate such a comparison. Hence it is reasonable to study first the deductions from the similarity theory alone, which are, moreover, interesting in their own right.

3. Experimental verification of similarity laws and similarity computation of velocity profiles

Ludwieg & Tillmann (1949) performed the best-known experiments which confirmed the applicability of the Prandtl wall law (2) and of the logarithmic law (3) to the wall region of a turbulent boundary layer in a moderate longitudinal pressure gradient. Similar experiments were repeated later by many other investigators and the validity of (2), (3) and (3a) for wall flows in a pressure gradient has now been confirmed very reliably (cf., for example, Perry *et al.* 1966; Coles & Hirst 1969; or Townsend 1976). The most widely used values of the constants in (3) are $A = 2{\cdot}5$ (i.e. $k = A^{-1} = 0{\cdot}4$) and $B = 5$; however, the scatter in the proposed values of these constants is still rather high. In fact, the widely used values of k and A vary, at least, from $k = 0{\cdot}35$ and $A = 2{\cdot}9$ (e.g. Businger *et al.* 1971) to $k = 0{\cdot}435$ and $A = 2{\cdot}3$ (e.g. Ng & Spalding 1976), but values far outside this range can also be found in the literature and the scatter in the values of B is even greater than that in the values of A. On the basis of the scatter in the values of A, Tennekes (1968) formulated some arguments in favour of the validity of the equation $A = A_0 - A_1(\delta_v/\delta_p)^{\frac{1}{4}}$, where $A_0 \approx 3$ and $A_1 \approx 4$, for turbulent tube flow (see also Tennekes & Lumley 1972, § 5.4). Tennekes' equation for A transforms (3) into a special case of (2a). This equation for A is, however, not universally recognized and moreover was recommended for a pressure-gradient tube flow only, i.e. for a special type of turbulent wall flow with $\alpha < 0$.† Therefore we shall use below only the usual equation (3) with constant coefficients A and B. Moreover we shall follow the recommendations of Coles & Hirst (1969) and assume that $A = 2{\cdot}44$ (i.e. $k = 0{\cdot}41$) and $B = 5$.

Many forms of the wall-law function $\phi_1(y_+)$ and the related velocity-profile function

$$\Phi_1(y_+) = \int_0^{y_+} \phi_1(y')\, y'^{-1} dy'$$

† It is easy to verify that for tube flow $\alpha = -2u_*^2/\delta$, where δ is the tube radius, and hence $\delta_p = \frac{1}{2}\delta$.

can be found in the literature (see, for example, Monin & Yaglom 1971, §5.3; or Hinze 1975, §7.5). These forms seem to be quite different, but in fact they are rather close to each other. All of the forms are based on some interpolation function which makes a smooth junction with the logarithmic equation for $U(y)$ at $y_+ = yu_*/\nu \gg 1$ and with the linear equation $U(y) = u_*^2 y/\nu$ at $y_+ \ll 1$. Moreover all the suggested forms of $\phi_1(y_+)$ and $\Phi_1(y_+)$ agree with the existing experimental data to approximately the same degree of accuracy. In the present paper we shall use, for definiteness, the equation

$$\frac{U(y)}{u_*} = \Phi_1(y_+) = \begin{cases} 14{\cdot}5 \tanh(y_+/14{\cdot}5) & \text{for} \quad 0 < y_+ < 27{\cdot}5, \\ 2{\cdot}44 \ln y_+ + 5 & \text{for} \quad y_+ > 27{\cdot}5. \end{cases} \tag{10}$$

Equation (10) is one of the simplest recommendations for $\Phi_1(y_+)$; it is mentioned, for example, by Hinze (1975) and it is rather widely used (cf. McDonald 1969; or Schofield & Perry 1972).

Townsend (1961, 1976), Mellor (1966), McDonald (1969) and some other authors proposed refined equations for the velocity profile near the wall. In these equations, the influence of $\alpha = \rho^{-1} dP/dx$ is taken into account with the help of the replacement of the usual wall law by a special form of (2*a*). The above-mentioned authors used both experimental data and semi-empirical hypotheses to derive the proposed profile equations. The graphs of the recommended functions

$$\Phi_1(y_+, u_*^3/\alpha\nu) = \int_0^{y_+} \phi_1(y', u_*^3/\alpha\nu)\, y'^{-1}\, dy'$$

vs. the argument y_+ at various values of $u_*^3/\alpha\nu$ are shown in figure 5 of Mellor (1966) and in figure 2 of McDonald (1969). Both authors emphasize that the influence of the pressure gradient α can destroy the logarithmic layer of the flow when the value of $\delta_p/\delta_v = u_*^3/|\alpha|\nu$ is not high enough. The same influence can also lead to a velocity profile for $y_+ < 27{\cdot}5$ which is quite different from that of an idealized wall flow with $dP/dx = 0$ and $\tau(y) =$ constant. The last fact has some important physical implications. It is well known now that the turbulent energy production in turbulent wall flows has its maximum value within the so-called 'buffer region' between the logarithmic layer and the viscous sublayer, where the velocity profile is linear (see, for example, Hinze 1975, §7.13). If the pressure gradient is negative and high in absolute value (i.e. $u_*^3/|\alpha|\nu$ is small), the region of influence of α reaches the 'buffer region' of the flow; this influence leads to a considerable 'overshoot' in the velocity profile compared with (10) and to a decrease in turbulent production. As a result relaminarization (i.e reverse transition) may occur. Relaminarization is often observed in turbulent boundary layers subjected to strong favourable pressure gradients (see, for example, Patel & Head 1968; Badri Narayanan & Ramjee 1969; Bradshaw 1969; or Kreskovsky *et al.* 1975). The similarity arguments of the present paper imply that relaminarization must take place at moderate values of $\delta_p/\delta_v = u_*^3/|\alpha|\nu$, beginning at some 'critical' value of this parameter. This statement may be made even more precise: since the upper edge of the 'buffer region' is close to the plane $y = 50\nu/u_* = 50\delta_v$, it is natural to expect that the 'critical' value of the ratio δ_p/δ_v is of the order of a few dozen. This expectation agrees well with experimental data of Schraub & Kline (1965), Patel & Head (1968) and Badri Narayanan & Ramjee (1969) which show that relaminarization usually takes place at $u_*^3/|\alpha|\nu \approx 50$ (see also Bradshaw 1969).

In the case of an adverse pressure gradient (i.e. $\alpha > 0$), at moderate values of $u_*^3/\alpha\nu$ the influence of α also extends to the 'buffer region' and viscous sublayer. This influence changes the turbulent structure in the vicinity of the wall and can lead to separation of the flow. In fact the data of Schraub & Kline (1965) show that if $\alpha > 0$ then the number of 'bursts' in the viscous sublayer of the flow increases considerably from $u_*^3/\alpha\nu \approx 50$ onwards, i.e. from the same value of $u_*^3/|\alpha|\nu$ as characterizes relaminarization when $\alpha < 0$. The intensification of bursting leads at first to the appearance of local separations of the flow, i.e. to the beginning of the so-called intermittent or turbulent separation (see, for example, Sandborn & Kline 1961), and then (at the point where u_* vanishes) to permanent, fully developed separation. The above arguments lead us to expect that the value $u_*^3/\alpha\nu = 50$ will, apparently, give a rough estimate of the point at which intermittent separation (i.e. near-separation flow) begins.

The use of a more complicated equation for $\partial U/\partial y$ (or $U(y)$) depending on the dimensionless parameter $u_*^3/|\alpha|\nu$ instead of (10) may, apparently, allow one to obtain slightly better agreement with velocity-profile data in the vicinity of a wall. However, in this paper we are trying to describe the whole velocity profile with satisfactory accuracy and are not interested in obtaining the best possible fit to the data within particular narrow layers. Therefore we shall base our analysis on the known fact of the satisfactory applicability of the usual wall law (2) even when $u_*^3/|\alpha|\nu$ is relatively small (Coles & Hirst 1969) and shall not consider forms of the wall law which are more complicated than (10). Nevertheless the value of $u_*^3/\alpha\nu$ will influence significantly the velocity distribution in the vicinity of a wall according to our theory too. However, this influence will not be related to the change in the form of the wall law, but will change the range of y values in the region of applicability of (10).

The gradient layer of a flow with a velocity gradient of the form (4) lies just above the region of validity of the universal law (2). Equation (4) is similar to the well-known equation of Monin and Oboukhov for the velocity gradient in a thermally stratified turbulent wall flow; the only difference is that the pressure-gradient length scale δ_p is used in (4) instead of the Oboukhov stratification length scale L (see, for example, Monin & Yaglom 1971, chap. 4). The equation related to (4) was indicated in a note by Engelund (1973), which also contains the only attempt known to us to estimate roughly the form of $\phi_2(\zeta)$ (or, more precisely, the deviation of the indefinite integral of $\phi_2(\zeta)\zeta^{-\frac{1}{2}}$ from the logarithmic function) from measurements in pressure-gradient wall flows. Engelund's approach to the theory of pressure-gradient flows is similar to the approach of the present paper, but his results for the form of the velocity profile are not reliable enough and need further verification and refinement. However, we shall not dwell upon this problem here. The reason is that the fluid layer where the usual wall law (2) is inapplicable and at the same time the 'half-power law' is also invalid is usually very thin according to all the data analysed below. Therefore in most cases this layer can be neglected when one computes the velocity profile in a pressure-gradient boundary layer.

Let us now consider the 'half-power layer' of the flow where the velocity profile may be described by the 'half-power law' (6) with a satisfactory accuracy. This layer plays a very important part in our analysis. The 'half-power law' (6) was apparently first suggested in 1956 in unpublished work by the Moscow scientists E. E. Solodkin and I. I. Mezhirov (see Ginevskii 1969, p. 275). The classical mixing-length theory of

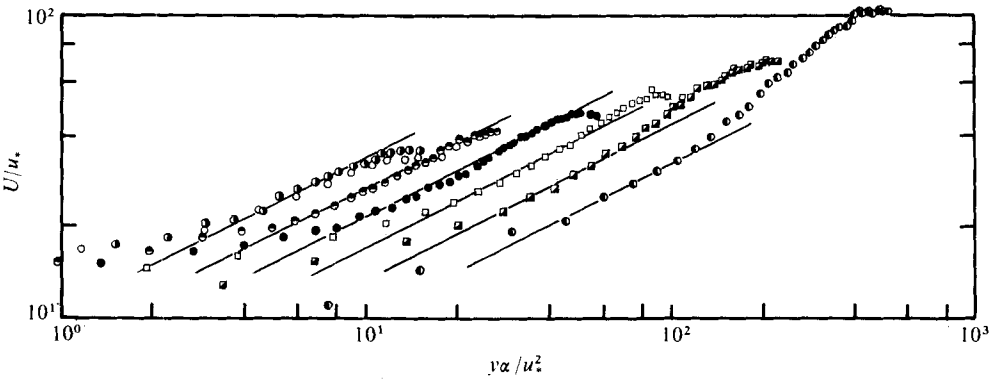

FIGURE 1. Dimensionless velocity profiles of Newman's (1951) airfoil boundary layer at different values of the streamwise co-ordinate x. Values of x (in metres): ○, 0·61; ◑, 0·84; ◓, 1·07; ●, 1·22; □, 1·37; ◪, 1·45; ◐, 1·50. The solid lines correspond to the relationship $U(y)/u_* \propto (y\alpha/u_*^2)^{\frac{1}{2}}$.

Prandtl was applied in this work to a wall flow with a linear shear stress profile $\tau(y)$ and it was also assumed that the mixing length was proportional to the distance from the wall. In other words the method used by Prandtl to derive the logarithmic law (3) was applied by Solodkin & Mezhirov to derive the 'half-power law'. The first published papers containing the derivation of the 'half-power law' are those by Ginevskii & Solodkin (1958) and Stratford (1959*a*). We mention that Stratford gave a purely dimensional derivation of the 'half-power law' in addition to the mixing-length derivation, i.e. he supplemented the Prandtl mixing-length arguments by arguments similar to those used by Landau & Lifshitz (1963, chap. 4) to obtain the logarithmic law (3).† The paper by Stratford (1959*a*) includes also a reference to his adjacent experimental paper (Stratford 1959*b*), where the 'half-power law' is verified for an artificial pressure-gradient boundary layer with negligible wall stress.

Stratford's work (1959*a*, *b*) attracted much attention and stimulated the appearance of many subsequent theoretical and experimental investigations of the 'half-power law' (see, for example, Townsend 1960, 1961; Perry *et al.* 1966; McDonald 1969). In particular, Perry *et al.* gave a very clear presentation of the dimensional derivation of the 'half-power law' and also made special measurements which imply (together with some previous measurements by different authors) that the constant $\mathscr{K}$ in (6) is about 4·16. The same value of the constant $\mathscr{K}$ is given in the recent book by Townsend (1976, § 5.15). However, Schofield & Perry (1972) and Perry & Schofield (1973) made a very careful treatment of all the velocity profiles of boundary layers in adverse pressure gradients from the book by Coles & Hirst (1969) and found that, in fact, the situation is more complicated than was supposed by Perry *et al.* (1966). To illustrate the real situation we plot in figure 1 logarithmic graphs of the quite typical data of Newman (1951) for velocity profiles in an airfoil boundary layer. Figure 1 shows that a considerable region of proportionality of $U(y)$ to $(\alpha y)^{\frac{1}{2}}$ can be found in all the boundary-layer cross-sections. However the corresponding factor of proportionality is not

† The first Russian edition of Landau & Lifshitz' book containing the dimensional derivation of the logarithmic law was published in 1944. We also remark that the derivation of the 'half-power law' with the aid of 'overlap layer arguments' given in § 1 of the present paper is completely analogous to Izakson's (1937) derivation of the logarithmic law.

constant but takes different values in different cross-sections. Schofield & Perry (1972) treated the data from 11 experiments containing 145 velocity-profile measurements for boundary layers in adverse pressure gradients and found that the situation shown in figure 1 is a very usual one. In fact all the profiles treated contain a region of validity of the 'half-power law', but the values of the dimensionless coefficient $\mathscr{K}$ in (6) are very far from being constant and show a large spread. Therefore it seems that the experimental data clearly contradict the similarity law (6) since the coefficient $\mathscr{K}$ in this law must be strictly constant according to the deductions from the dimensional analysis. That is why Schofield & Perry (1972) and Perry & Schofield (1973) deduced that the assumption that the local values u_* (or U_∞), δ and α are the only physical quantities which determine the velocity profile in any fixed cross-section of a boundary layer could not be correct. Instead of this assumption they introduced some alternative length and velocity scales that were determined in a special manner from the velocity and shear stress profiles $U(y)$ and $\tau(y)$ at the given value of x.

Let us try to apply another argument to explain Schofield & Perry's finding. In fact, their results do not necessarily imply that the list of physical parameters which determine the flow conditions at the fixed value of x must be extended compared with the list given in § 2 of the present paper. The variations in $\mathscr{K}$ found by Schofield & Perry may indicate that the values of the dimensionless parameter $\delta/\delta_p = \alpha\delta/u_*^2$ were not large enough in the experiments analysed to guarantee the applicability of the limiting law (6), which is derived for the situation when $\alpha\delta/u_*^2 \to \infty$. It is easy to verify that the values of $\alpha\delta/u_*^2$ for most of the data from the book by Coles & Hirst (1969) do not exceed several tens, i.e. are not very high. (Let us recall for comparison that the lower edge of the logarithmic layer is often supposed to be located at a distance y which exceeds the viscous length scale $\delta_v = \nu/u_*$ by many tens of times.) The formulated explanation of the finding of Schofield & Perry means that most of the data analysed are related to turbulent flows in which the corresponding velocity gradient $\partial U/\partial y$ is described within the gradient layer by the general equation (4*a*) and not by the special case (4) of (4*a*). Of course, it is possible that within the region of applicability of (4*a*) a sublayer may be found in which the velocity gradient is described with satisfactory accuracy by the relation $\partial U/\partial y \propto y^{-\frac{1}{2}}$. It is necessary for this that the function $\phi_2(y\alpha/u_*^2, \alpha\delta/u_*^2)$ should vary only slowly with its first argument $y\alpha/u_*^2$ in the indicated sublayer. In other words it is necessary that the function should not change appreciably with y, i.e. should be approximated by a function of the single variable $\alpha\delta/u_*^2$ with satisfactory accuracy. It is natural to assume that such a situation arises within the 'half-power layers' of most of the flows considered by Schofield & Perry. If this is really so, then the velocity profile within the indicated 'half-power layers' must be described by an equation of the form

$$\partial U/\partial y = \tfrac{1}{2}\mathscr{K}(\alpha\delta/u_*^2)\,(\alpha/y)^{\frac{1}{2}}, \quad U(y) = \mathscr{K}(\alpha\delta/u_*^2)\,(\alpha y)^{\frac{1}{2}} + \mathscr{K}_1, \tag{11}$$

where $\mathscr{K}(\alpha\delta/u_*^2)$ is a function of $\alpha\delta/u_*^2$. It is clear that the law (11) is a generalization of the usual 'half-power law' (6). Hence we shall call the law (11) and the layer in which it is valid the 'generalized half-power law' and 'generalized half-power layer', respectively.

On the basis of the above assumption we treat anew all the data analysed by Schofield & Perry. Initially we suppose that $\mathscr{K}_1 = 0$ since this simplifies considerably

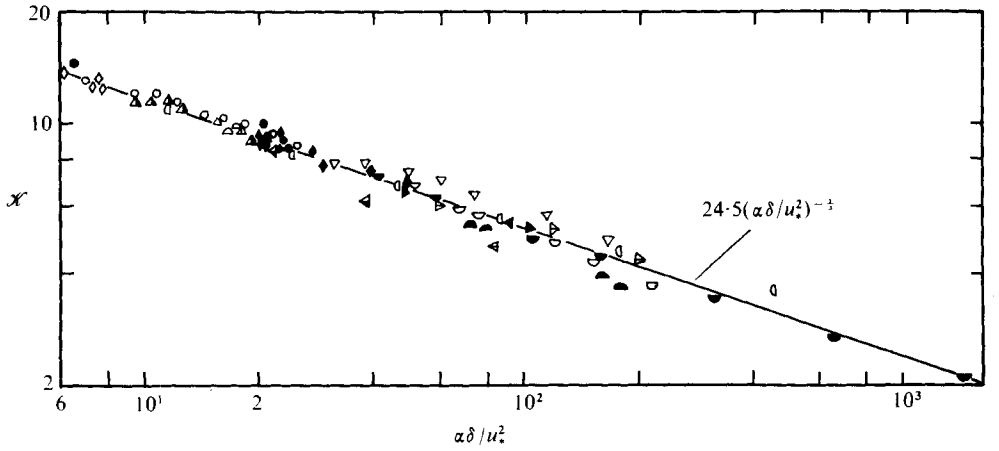

FIGURE 2. Dependence of the coefficient $\mathscr{K}$ in the 'half-power law' on $\alpha\delta/u_*^2$ according to experimental data. Number of experiment in Coles & Hirst (1969): ○, 1100; ●, 1200; ◇, 2200; ◆, 2300; △, 2400; ⧋, 2600; ▽, 2900; ▲, 3300; ◖, 3500; ◀, 3700; ◁, 3800; ◁, 4000; ▶, 4500; ▷, 4800; ⊍, 5000; ◒, 5100; ◓, 5200; ⌓, 5300.

the isolation of the 'generalized half-power layer' in the logarithmic graph of $U(y)$. Moreover, we supplement our treatment by plotting the dependence of $\mathscr{K}$ on the parameter $\alpha\delta/u_*^2$ (see figure 2). The results obtained are very convincing: all the experimental points lie very close to a single smooth curve which can be described by the simple power law

$$\mathscr{K}(\alpha\delta/u_*^2) = 24{\cdot}5(\alpha\delta/u_*^2)^{-\frac{1}{8}}. \tag{12}$$

Therefore it is natural to suppose that the strong variations in the values of $\mathscr{K}$ in Schofield & Perry (1972) and in Perry & Schofield (1973) are also due to the dependence of $\mathscr{K}$ on $\alpha\delta/u_*^2$, which is disregarded by these authors.

The equation $U(y) = \mathscr{K}(\alpha y)^{\frac{1}{8}}$, where $\mathscr{K} = \mathscr{K}(\alpha\delta/u_*^2)$ is given by (12), permits one to describe rather precisely a considerable portion of any of the velocity profiles $U(y)$ analysed by Schofield & Perry. If we combine this equation with other similarity equations from the present paper, we may obtain a satisfactory description of all the profiles over the whole range of y from $y = 0$ to $y = \delta$. The power law (12) for $\mathscr{K}$ agrees well with the well-known frequent appearance of power-law relations in various branches of continuum mechanics (see, for example, Barenblatt & Zel'dovich 1972; Barenblatt 1976, where the special term 'self-similarity of the second type' was introduced for such relations). However, such 'self-similarity of the second type' usually occurs as an intermediate asymptotic regime which is transformed into the usual 'self-similar equilibrium regime' as a dimensionless parameter of the problem tends to infinity. The main difference between the usual self-similarity ('self-similarity of the first type') and 'self-similarity of the second type' is that the dimensionless exponents in the corresponding power-law relations can be determined from dimensional analysis only in case of 'self-similarity of the first type'. Therefore it seems natural to expect that the function $\mathscr{K}(\alpha\delta/u_*^2)$ will tend to a constant value as $\alpha\delta/u_*^2 \to \infty$. The lack of such a tendency in figure 2 may be related, for example, to the introduction of the supplementary assumption that $\mathscr{K}_1 = 0$. (This supplementary assumption simplifies the treatment of the data but has no physical basis.) Therefore

we have treated again all the velocity-profile data for adverse-pressure-gradient boundary layers from Coles & Hirst (1969) (and also the later data of Samuel & Joubert 1974) without using any assumption about $\mathscr{K}_1$. We base our new treatment on the values of $\partial U/\partial y$ and use a computer for the determination of the regions of applicability of the first equation (11), which does not include $\mathscr{K}_1$. Compared with the treatment by Schofield & Perry and with our old treatment, the new treatment leads to a considerable extension of the set of profiles $U(y)$ with a definite 'generalized half-power layer' and of the ranges of y values within these layers. In particular, the 'generalized half-power law' now proves to be applicable to many profiles $U(y)$ with $\alpha\delta/u_*^2 \lesssim 1$, although the usual derivation of the law is based on the assumption that $\alpha\delta/u_*^2 \gg 1$. (This is clearly due to the fact that it is very often possible to find a narrow range of y where the equation $U(y) = k_1 y^{\frac{1}{2}} + k_2$ is valid with satisfactory accuracy.) The collection of new values of $\mathscr{K}$ is plotted in figure 3 as a function of $\alpha\delta/u_*^2$. We see that the new values are also described satisfactorily by a single-valued function of $\alpha\delta/u_*^2$. (The increase in the scatter in figure 3, compared with figure 2, may be explained, for example, by the influence of errors due to the differentiation of $U(y)$.) However the new function $\mathscr{K}(\alpha\delta/u_*^2)$ may be described by a power law (of the form $\mathscr{K}(\alpha\delta/u_*^2) = 14(\alpha\delta/u_*^2)^{-\frac{1}{2}}$) only provided that $\alpha\delta/u_*^2$ is not too large. As $\alpha\delta/u_*^2$ increases the rate of decrease of $\mathscr{K}(\alpha\delta/u_*^2)$ decreases and the function $\mathscr{K}$ tends to a constant value as $\alpha\delta/u_*^2 \to \infty$. In fact, the values of $\mathscr{K}$ are practically constant in the range $\alpha\delta/u_*^2 > 50$ and the limiting value of $\mathscr{K}$ is close to 4·5, i.e. it differs slightly from the value of $\mathscr{K}$ recommended by Perry *et al.* (1966) and by Townsend (1976, § 5.15). Hence the results of the new treatment show that the 'generalized half-power law' corresponds, apparently, to 'self-similarity of the second type' at small values of $\alpha\delta/u_*^2$ (say $\alpha\delta/u_*^2 \leqslant 5$) and to the usual 'self-similarity of the first type' at large values of $\alpha\delta/u_*^2$ ($\alpha\delta/u_*^2 > 50$).

The function $\mathscr{K}(\alpha\delta/u_*^2)$ may be described over the whole range of $\alpha\delta/u_*^2$ by an interpolation equation which joins smoothly with the power law $\mathscr{K} = \mathscr{K}' \times (\alpha\delta/u_*^2)^{-\frac{1}{2}}$ as $\alpha\delta/u_*^2 \to 0$ and tends to a constant $\mathscr{K}''$ as $\alpha\delta/u_*^2 \to \infty$. The simplest interpolation equation has the form of a linear relation $\mathscr{K} = \mathscr{K}'(u_*^2/\alpha\delta)^{\frac{1}{2}} + \mathscr{K}''$, which is similar to the equation for the coefficient A of the logarithmic law recommended by Tennekes (1968). An equation for $\mathscr{K}$ of such a form was used in the preliminary version of the present paper (Kader & Yaglom 1977*b*). However, a more complicated interpolation equation of the form

$$\mathscr{K} = \{[\mathscr{K}' \times (u_*^2/\alpha\delta)^{\frac{1}{2}}]^m + (\mathscr{K}'')^m\}^{1/m}$$

may be also used and an increase in the exponent m leads to more distinct separation of the asymptotic behaviour of $\mathscr{K}(\alpha\delta/u_*^2)$ at large and small values of $\alpha\delta/u_*^2$. Figure 3 shows that fully satisfactory agreement with the data can be achieved if we select $m = 2$ and take

$$\mathscr{K} = (200u_*^2/\alpha\delta + 20)^{\frac{1}{2}}. \tag{13}$$

This equation for $\mathscr{K}$ will be used below.

The constant $\mathscr{K}_1$ represents the velocity of slip at the wall, if the half-power equation is extrapolated to the wall; we shall call it the 'slip velocity'. The experimental value of the slip velocity may be determined easily if the value of $\mathscr{K}$ is known. Instead of extrapolating the graph of the 'generalized half-power law' to the wall it is more convenient to use a computer to determine $\mathscr{K}_1$. It is necessary for this only to compute

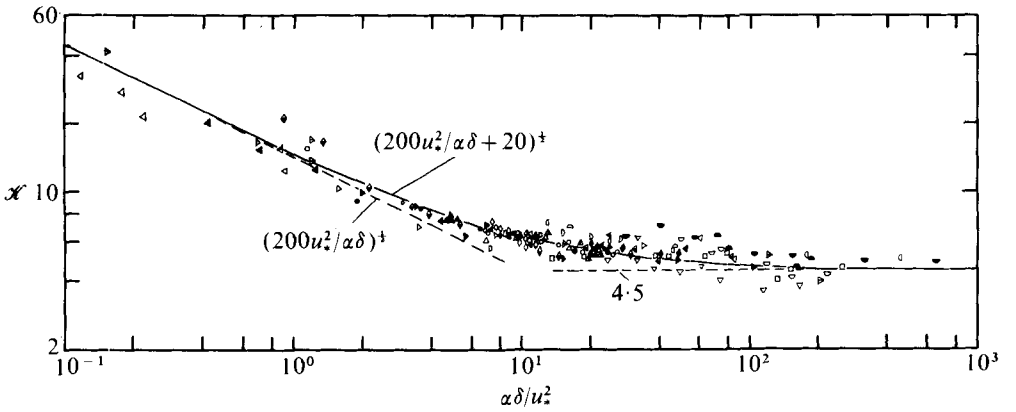

FIGURE 3. Refined data on the dependence of $\mathscr{K}$ on $\alpha\delta/u_*^2$. The symbols appearing also in figure 2 have the same meaning here. Number of experiment in Coles & Hirst (1969): □, 2100; ▲, 2500; D, 3200; ◁, 3600; ◀, 4100; ▷, 4400. ◆, Samuel & Joubert's data (1974). All the symbols used in figures 1 and 2 have the same meaning in the subsequent figures.

the difference $U(y)-\mathscr{K}(\alpha y)^{\frac{1}{2}}$ for all the y values within the generalized half-power layer and then to form the arithmetic mean of all the values of the difference related to a given profile $U(y)$. The values of the dimensionless slip velocity $\mathscr{K}_1/u_*$ obtained are plotted in figure 4 *vs.* the variable Γ, which appears when we try to obtain a crude theoretical estimate of $\mathscr{K}_1$. This estimate is based on the simplified assumption of a smooth junction (without a jump in the values of $\partial U/\partial y$) between the 'generalized half-power law' (11) and the wall law (10). Let us suppose at first that the junction occurs within the logarithmic layer, i.e. at $y_+ \geqslant 27{\cdot}5$, where $U(y)/u_* = 2{\cdot}44\ln y_+ + 5$. We assume that $2{\cdot}44\ln y_+ + 5 = \mathscr{K}(\alpha y/u_*^2)^{\frac{1}{2}} + \mathscr{K}_1/u_*$ and $2{\cdot}44/y = 0{\cdot}5\mathscr{K}(\alpha/yu_*^2)^{\frac{1}{2}}$ at the junction. Then it is easy to show that

$$\frac{\mathscr{K}_1}{u_*} = 2{\cdot}44\ln\Gamma, \quad \Gamma = \frac{u_*^3}{\alpha\nu}\frac{(4{\cdot}88)^2}{\mathscr{K}^2} \approx \frac{6u_*^3/\alpha\nu}{5(1+10u_*^2/\alpha\delta)}. \tag{14}$$

However, the logarithmic layer does not exist at very high values of $\alpha\nu/u_*^3$. At high enough values of $\alpha\nu/u_*^3$ (i.e. at small enough values of Γ) the junction will occur within the viscous sublayer, where $U(y) = u_*^2 y/\nu$. Therefore the equations

$$u_* y/\nu = \mathscr{K}(\alpha y/u_*^2)^{\frac{1}{2}} + \mathscr{K}_1/u_*, \quad u_*/\nu = 0{\cdot}5\mathscr{K}(\alpha/yu_*^2)^{\frac{1}{2}}$$

must be valid at very small values of Γ, and these equations imply that

$$\mathscr{K}_1/u_* = -(4{\cdot}88)^2/4\Gamma \approx -6/\Gamma, \tag{14a}$$

where Γ has the same meaning as in (14). Hence the function $\mathscr{K}_1(\Gamma)/u_*$ must be described by the asymptotic equation (14) at large values of Γ and by (14*a*) at small values of Γ. Figure 4 shows that the existing experimental values of $\mathscr{K}_1/u_*$ may be approximated satisfactorily by the interpolation equation

$$\frac{\mathscr{K}_1}{u_*} = 2{\cdot}44\ln\Gamma - \frac{15}{\Gamma^{\frac{1}{2}}} - \frac{6}{\Gamma}, \quad \Gamma = \frac{6u_*^3/\alpha\nu}{5+50u_*^2/\alpha\delta}, \tag{15}$$

which agrees with both the asymptotic equations (14) and (14*a*); one more term $-15/\Gamma^{\frac{1}{2}}$ is included in the right-hand side of (15) to achieve better agreement with the data.

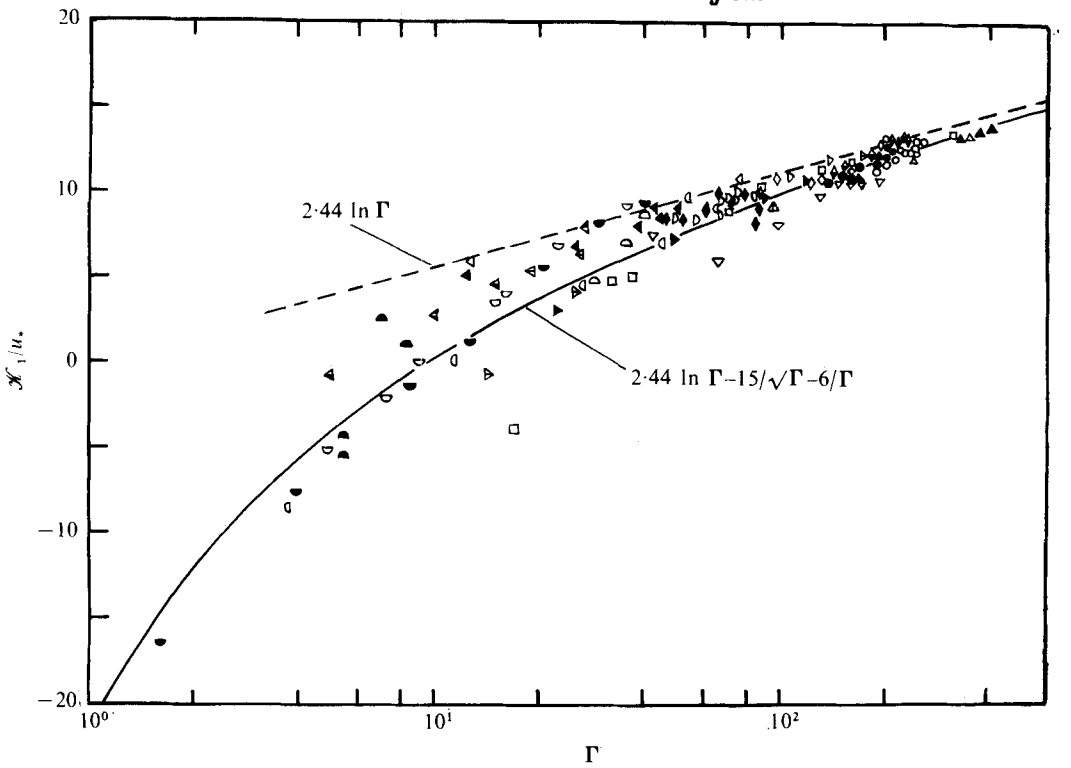

FIGURE 4. The dependence of the coefficient $\mathscr{K}_1$ on the parameter Γ according to experimental data.

It has already been indicated at the end of § 1 that the 'half-power layer' coincides with the overlap layer where the gradient law (4) and the velocity defect law (7) are valid simultaneously. However we have considered in § 1 only the form (6) of the 'half-power law' where the coefficients are constant. Now we see that most of the data from the book by Coles & Hirst do not agree with the 'half-power law' (6) but do agree, over some range of y values, with the generalized half-power law (11), which is a special case of the generalized gradient law (4a). It is easy to see that the first of equations (11) is also a special case of the first of equations (7a) corresponding to a function ϕ_3 of the form $\phi_3(y/\delta, \alpha\delta/u_*^2) = 0{\cdot}5(y/\delta)^{\frac{1}{2}}\mathscr{K}(\alpha\delta/u_*^2)$. Therefore the region of applicability of the 'generalized half-power law' (11) coincides with the overlap layer where the generalized gradient law (4a) and the generalized velocity defect law (7a) are valid simultaneously. The above-mentioned equation for $\phi_3(\eta, s)$ implies that the velocity defect law (7a) must have the form

$$[U_\infty - U(y)]/(\alpha\delta)^{\frac{1}{2}} = -\mathscr{K}(\alpha\delta/u_*^2)\,(y/\delta)^{\frac{1}{2}} + I(\alpha\delta/u_*^2) \tag{16}$$

within the overlap layer. As in the case of (9), the function $I(\alpha\delta/u_*^2)$ can be roughly estimated with the aid of the assumption that the region of applicability of (16) extends to the upper edge of the boundary layer. This assumption implies that $I(\alpha\delta/u_*^2) \approx \mathscr{K}(\alpha\delta/u_*^2)$. Therefore we plot equation (13) for $\mathscr{K}$ in figure 5 together with the experimental values of $I(\alpha\delta/u_*^2)$. The values of the term $I(\alpha\delta/u_*^2)$ of (16) are determined here by the method which has been used above to determine the experimental values of the term $\mathscr{K}_1$ of (11). We see that all the values of $I(\alpha\delta/u_*^2)$ are close

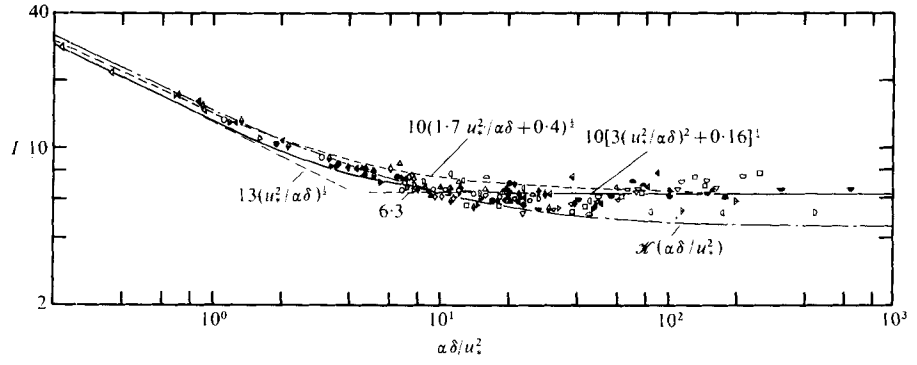

FIGURE 5. The dependence of I on $\alpha\delta/u_*^2$.

to a single curve but that they deviate significantly from the values of $\mathscr{K}(\alpha\delta/u_*^2)$. This is not at all surprising, since the estimate $I(\alpha\delta/u_*^2) \approx \mathscr{K}(\alpha\delta/u_*^2)$ is not precise.

The equation $I(\alpha\delta/u_*^2) = 10[1{\cdot}7u_*^2/\alpha\delta + 0{\cdot}4]^{\frac{1}{2}}$, represented by a dashed curve in figure 5, fits the data better than does (13); however, the data are described even more precisely by the equation

$$I(\alpha\delta/u_*^2) = 10[3u_*^4/(\alpha\delta)^2 + 0{\cdot}16]^{\frac{1}{4}}. \tag{17}$$

This equation will be used below. Equation (17) leads to the asymptotic laws

$$I \approx 13u_*/(\alpha\delta)^{\frac{1}{2}}, \quad I \approx 6{\cdot}3 = \text{constant}$$

at small and large values of $\alpha\delta/u_*^2$ respectively. Both these asymptotic laws are also plotted in figure 5 and will be discussed later.

Let us now consider the velocity defect laws (7) and (7a). The law (7) differs from the usual velocity defect law for boundary layers (see, for example, Monin & Yaglom 1971; Hinze 1975; Townsend 1976) by the replacement of the velocity scale u_* by the velocity scale $(\alpha\delta)^{\frac{1}{2}}$. The uselessness of the velocity scale u_* for the description of the outer part of a boundary layer at large values of $\delta/\delta_p = \alpha\delta/u_*^2$ (i.e. at large α or small u_*) is emphasized in some previous papers too. For example, Mellor & Gibson (1966) suggested the replacement of the velocity scale u_* by $(\alpha\delta^*)^{\frac{1}{2}}$, where δ^* is the displacement thickness, when the parameter $\beta = \alpha\delta^*/u_*^2$ was large. (At moderate values of β, Mellor & Gibson used the usual velocity scale u_*. Nevertheless they modified the usual velocity defect law by replacing the length scale δ by a related but different length scale at each value of β.) For the special case of negligible wall stress Chawla & Tennekes (1973) suggested the law $[U_\infty - U(y)]/U_\infty = \Phi(y/\delta)$, i.e. they used the free-stream velocity U_∞ as the velocity scale in the velocity defect law. Schofield & Perry (1972) and Perry & Schofield (1973) also modified the usual form of the velocity defect law for a wide collection of boundary layers in adverse pressure gradients. These authors introduced special velocity and length scales which were determined by the mean velocity variations within the outer part of the boundary layer and were independent of the value of u_*. However, the simple velocity defect equation (7) seems to be most natural from the point of view of the general similarity and dimensional arguments of the present paper.

We have already seen that the velocity gradient is usually dependent on the values of the parameter $\delta/\delta_p = \alpha\delta/u_*^2$ within the generalized half-power layer. Therefore it

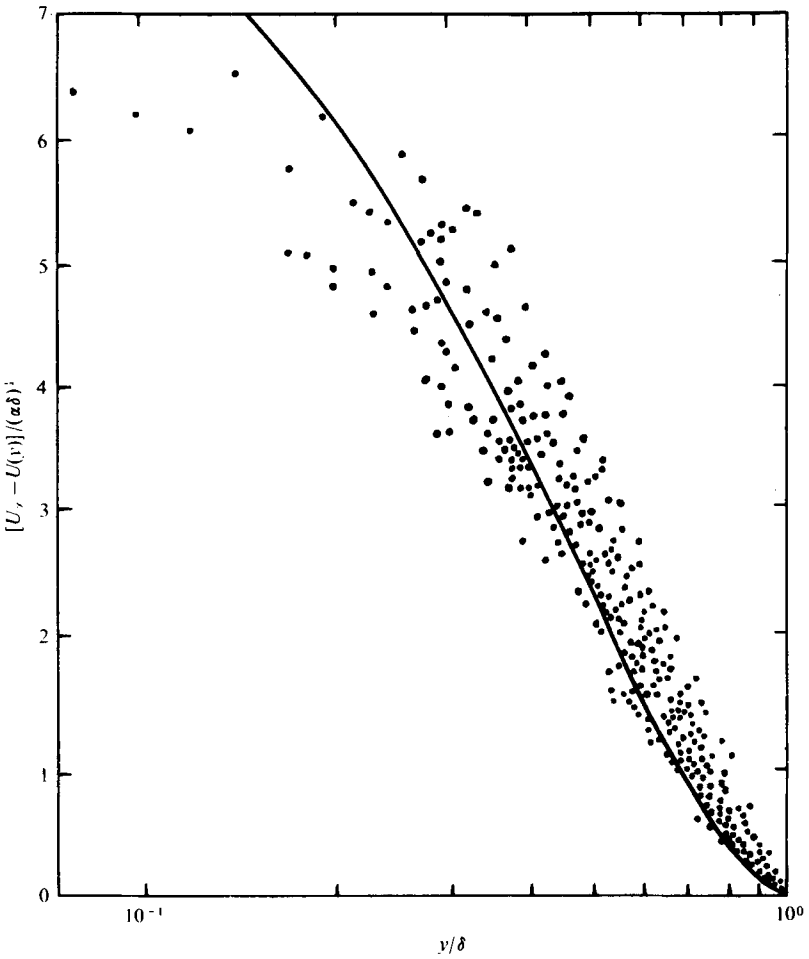

FIGURE 6. Dimensionless velocity defect as a function of y/δ for all the velocity profiles from Coles & Hirst (1969) corresponding to $\alpha\delta/u_*^2 > 50$. The solid line represents equation (18).

is natural to suppose that the same parameter influences the velocity distribution above this layer too. If this is true, then the velocity defect law cannot have the simple form (7), and must evidently have the generalized form (7*a*). Within the generalized half-power layer the form of $\Phi_3(\eta, \alpha\delta/u_*^2)$ is given by (16), i.e. it depends on two functions $\mathscr{K}(\alpha\delta/u_*^2)$ and $I(\alpha\delta/u_*^2)$ of one variable. However, there is no reason to expect that this equation is valid at large values of $\eta = y/\delta$ including the neighbourhood of the point $\eta = 1$ (i.e. at $y \approx \delta$). Hence we must consider $\Phi_3(\eta, \alpha\delta/u_*^2)$ in this region as an unknown function of two variables. Of course, the experimental determination of a function of two variables is a much more difficult and unreliable task than the experimental determination of a function of one variable. Therefore it is reasonable to consider at first only the data at large enough values of $\alpha\delta/u_*^2$. It is natural to expect that the velocity defect function $\Phi_3(\eta, \alpha\delta/u_*^2)$ will be independent of $\alpha\delta/u_*^2$ if $\alpha\delta/u_*^2 > 50$ (this expectation is based on the data in figure 3, which show that $\mathscr{K}$ is practically constant for $\alpha\delta/u_*^2 > 50$). On this basis we plot in figure 6 the dependence of $[U_\infty - U(y)]/(\alpha\delta)^{\frac{1}{2}}$ on $\eta = y/\delta$ for all the velocity-profile data from Coles

& Hirst (1969) which correspond to $\alpha > 0, \alpha\delta/u_*^2 > 50$ and large values of η. The scatter of the experimental points in figure 6 is rather large, but we must keep in mind that these points represent the measured values of the ratio of two relatively small quantities (in comparison with the values of $U(y)$ and U_∞), that δ is rather difficult to measure precisely, and that flows with large values of $\alpha\delta/u_*^2$ are usually approaching separation. The last circumstance implies that U_∞, α and δ are here rapidly changing with x, which makes accurate measurements rather difficult. Therefore it is impossible to decide at present whether the scatter in the points in figure 6 is due only to experimental errors or whether it reflects also the violation of moving equilibrium (i.e. the influence of the upstream history) or, perhaps, the influence of the variations in $\alpha\delta/u_*^2$. In any case the absolute values of $U(y)$ will be represented with a good accuracy by any smooth curve drawn through the central part of the set of points in figure 6, since $U(y)$ is considerably greater than $U_\infty - U(y)$ at large values of η. The spread of the points permits one to select several reasonable forms for the curve, i.e. to select several different equations for the function $\Phi_3(\eta) = \Phi_3(\eta, \infty)$ which fit the data with almost the same accuracy. In particular, the data agree well with the assumption that $\Phi_3(\eta)$ can be described by Hama's equation

$$\Phi_3(\eta) = 9{\cdot}6(1-\eta)^2, \tag{18}$$

which was proposed for the velocity defect function of a boundary layer with constant pressure (see, for example, Monin & Yaglom 1971, p. 315; Hinze 1975, p. 631). Let us recall that Clauser (1956) emphasized the similarity of the velocity defect functions in constant-pressure boundary layers and in all variable-pressure equilibrium boundary layers. The wake law of Coles is also based on the observation that the dependence of the normalized velocity defect on $y/\delta = \eta$ is determined by the universal wake function $w(\eta)$ to within a constant factor Π which may depend on the velocity gradient (see, for example, Coles & Hirst 1969, pp. 1–45; Allan & Sharma 1974). The form of the wake function does not differ too much from Hama's form of velocity defect function (cf. figure 1 in Huang 1974). The similarity of the velocity defect function for all the adverse-pressure-gradient boundary layers plays an important part in the arguments of Schofield & Perry (1972) and Perry & Schofield (1973). This similarity is reflected in our theory by the fact that the dependence of $\Phi_3(\eta, \alpha\delta/u_*^2)$ on η is similar to that of Hama's function for $\alpha\delta/u_*^2 > 50$ and, as it will be shown below, for all the other values of $\alpha\delta/u_*^2$ too. However, the coincidence of the numerical factor 9·6 on the right-hand side of (18) with that in the corresponding equation of Hama must, of course, be considered as fortuitous.

Now we have determined the asymptotic form of $\Phi_3(\eta, \alpha\delta/u_*^2)$ at $\alpha\delta/u_*^2 \to \infty$ and we also know the form of this function at $\alpha\delta/u_*^2 = 0$ (i.e. for a turbulent boundary layer with a constant pressure). Therefore we can try to choose an approximate form of $\Phi_3(\eta, \alpha\delta/u_*^2)$ for all values of $\alpha\delta/u_*^2$ by means of a simple interpolation between two asymptotes. It is convenient to begin by rewriting Hama's velocity defect law for a constant-pressure boundary layer in the following form:

$$\Phi_3(\eta, \alpha\delta/u_*^2) = 9{\cdot}6u_*(\alpha\delta)^{-\frac{1}{2}}(1-\eta)^2 \quad \text{for} \quad \alpha\delta/u_*^2 = 0. \tag{19}$$

The simplest interpolation equation joining (18) and (19) has the form

$$\Phi_3(\eta, \alpha\delta/u_*^2) = 9{\cdot}6\{1 + [u_*(\alpha\delta)^{-\frac{1}{2}}]^m\}^{1/m}(1-\eta)^2. \tag{20}$$

We may select any positive value of the exponent m in (20), and the transition to the asymptotic forms (18) and (19), when $\alpha\delta/u_*^2 \to \infty$ or $\alpha\delta/u_*^2 \to 0$, will be sharper the higher the value of m (cf. the derivation of equation (13) for $\mathscr{K}$). Comparison of (20) with experimental data shows that satisfactory results can be achieved if the value $m = 2$ is selected, i.e. the situation is fully analogous to that related to (13). Hence we may assume that

$$[U_\infty - U(y)]/(\alpha\delta)^{\frac{1}{2}} = \Phi_3(\eta, \alpha\delta/u_*^2) = 9{\cdot}6(1 + u_*^2/\alpha\delta)^{\frac{1}{2}}(1-\eta)^2. \tag{21}$$

This equation for $\Phi_3(\eta, \alpha\delta/u_*^2)$ will be used below in this paper. (For simplicity, it is suggested in the note by Kader & Yaglom (1977*b*) that $m = 1$ in (20). Such a value of m yields slightly worse, but also acceptable, agreement with the data.)

Let us also note that (21) can be used to justify the approximate equation (17) for $I(\alpha\delta/u_*^2)$. It is clear that (21) will be applicable only at large enough (i.e. close enough to 1) values of $\eta = y/\delta$. When η decreases the form of $\Phi_3(\eta, \alpha\delta/u_*^2)$ will change and be transformed into (16) after some value $\eta = \eta_1$. In the first approximation it is reasonable to suggest that the function $\Phi_3(\eta, \alpha\delta/u_*^2)$ can be described by (21) till a value $\eta = \eta_1$ determined as the value of η at the intersection of the curves

$$\Phi_3(\eta) = 9{\cdot}6(1 + u_*^2/\alpha\delta)^{\frac{1}{2}}(1-\eta)^2 \quad \text{and} \quad \Phi_3(\eta) = -\mathscr{K}(\alpha\delta/u_*^2)\,\eta^{\frac{1}{2}} + I(\alpha\delta/u_*^2),$$

while $\Phi_3(\eta, \alpha\delta/u_*^2)$ can be described by (16) at $\eta < \eta_1$. In other words it is reasonable to suggest that equations (21) and (16) for the velocity defect match each other directly at $\eta = \eta_1$. (This approximation has, apparently, a rather high accuracy.) If this is so, then evidently

$$I(\alpha\delta/u_*^2) = 9{\cdot}6(1 + u_*^2/\alpha\delta)^{\frac{1}{2}}(1-\eta_1)^2 + \mathscr{K}(\alpha\delta/u_*^2)\,\eta_1^{\frac{1}{2}},$$

where η_1 is the ordinate of the intersection point of the graphs of functions (21) and (16). Unfortunately, we do not know the exact value of η_1. However, it appears that the function $9{\cdot}6(1 + u_*^2/\alpha\delta)^{\frac{1}{2}}(1-\eta_1)^2 + \mathscr{K}(\alpha\delta/u_*^2)\,\eta_1^{\frac{1}{2}} = \mathscr{J}(\eta_1, \alpha\delta/u_*^2)$ does not change very much over a rather wide range of η_1. In fact, at first let us consider the case $\alpha\delta/u_*^2 \gg 1$, when $\mathscr{K}(\alpha\delta/u_*^2) \approx 4{\cdot}5$ and $\mathscr{J}(\eta_1, \alpha\delta/u_*^2) \approx 9{\cdot}6(1-\eta_1)^2 + 4{\cdot}5\eta_1^{\frac{1}{2}}$. The data in figure 6 show that the values of $\Phi_3(\eta, \infty)$ begin to deviate significantly from $9{\cdot}6(1-\eta)^2$ only when $\eta \approx 0{\cdot}3$–$0{\cdot}5$. The value of $9{\cdot}6\,(1-\eta_1)^2 + 4{\cdot}5\eta_1^{\frac{1}{2}}$ varies from 7·2 to 5·6 when η_1 varies from 0·3 to 0·5. Therefore we shall not incur a large error if we suggest that $I(\alpha\delta/u_*^2) = 9{\cdot}6(1-\eta_1)^2 + 4{\cdot}5\eta_1^{\frac{1}{2}}$ at $\eta_1 = 0{\cdot}4$, when $\alpha\delta/u_*^2 \gg 1$. Such an estimate shows that $I(\infty) \approx 6{\cdot}3$. Figure 6 clearly gives no possibility of estimating the value of η_1 in the second extreme case when $\alpha\delta/u_*^2 \ll 1$.† However, it appears that the function $\mathscr{J}(\eta_1,\ 0) \approx 9{\cdot}6u_*(\alpha\delta)^{-\frac{1}{2}}(1-\eta_1)^2 + (200\eta_1)^{\frac{1}{2}}\,u_*(\alpha\delta)^{-\frac{1}{2}}$ changes very slowly with η_1: the value of this function varies only from $12{\cdot}4u_*/(\alpha\delta)^{\frac{1}{2}}$ to $14u_*/(\alpha\delta)^{\frac{1}{2}}$ when η_1 varies from 0·2 to 1. Therefore we can assume that $I(\alpha\delta/u_*^2) \approx 13u_*/(\alpha\delta)^{\frac{1}{2}}$ for $\alpha\delta/u_*^2 \ll 1$ without taking the risk of making a large error. Figure 5 shows that both the asymptotic expressions for $I(\alpha\delta/u_*^2)$ derived above agree well with the experiments. We can now

† We can, however, use the data on the velocity defect in a constant-pressure turbulent boundary layer for this purpose. Such data, shown, for example, in figure 7-11 of Hinze (1975) and in figure 1 of Huang (1974), give the impression that the function $\Phi_3(\eta, 0)$ begins to deviate from the right-hand side of (19) at $\eta \approx 0{\cdot}3$–$0{\cdot}2$.

follow the method of obtaining the interpolation equations (13) and (21) for $\mathscr{K}(\alpha\delta/u_*^2)$ and $\Phi_3(\eta, \alpha\delta/u_*^2)$. This method leads to the interpolation equation

$$I(\alpha\delta/u_*^2) \approx 10(1{\cdot}7u_*^2/\alpha\delta + 0{\cdot}4)^{\frac{1}{2}}$$

for $I(\alpha\delta/u_*^2)$. However, figure 5 shows that this equation implies too smooth a transition from one asymptotic expression for $I(\alpha\delta/u_*^2)$ to the other. To make the transition sharper it is necessary to increase the exponent m in the interpolation equation analogous to (20). Figure 5 shows that the value $m = 4$, which corresponds to (17), gives good agreement with the data.

Let us now combine all the equations obtained to derive a description of the whole velocity profile $U(y)$ for adverse-pressure-gradient boundary layers. We shall consider the following three-layer model of the boundary layer. Very close to the wall there is a wall layer where the velocity profile is described by (10). (According to this equation the wall layer is decomposed into viscous and buffer sublayers for $y_+ < 27{\cdot}5$ and a logarithmic layer for $y_+ > 27{\cdot}5$.) The 'generalized half-power layer' is adjacent to the wall layer and the velocity profile within the new layer is described by the equivalent equations (11) and (16). Finally, far from the wall there is an outer turbulent layer where the velocity profile satisfies the generalized velocity defect law of the form (21). In other words we shall assume that the velocity profile at a given cross-section of a boundary layer is given by the equations:

$$\frac{U(y)}{u_*} = \begin{cases} 14{\cdot}5\tanh(yu_*/14{\cdot}5\nu) & \text{for } 0 < y < 27{\cdot}5\nu/u_*, \quad (22a) \\ 2{\cdot}44\ln(yu_*/\nu) + 5 & \text{for } 27{\cdot}5\nu/u_* < y < y_2, \quad (22b) \\ \mathscr{K}\dfrac{(\alpha\delta)^{\frac{1}{2}}}{u_*}\left(\dfrac{y}{\delta}\right)^{\frac{1}{2}} + \dfrac{\mathscr{K}_1}{u_*} & \text{for } y_2 < y < y_1, \quad (22c) \\ \dfrac{U_\infty}{u_*} - 9{\cdot}6\left(1 + \dfrac{\alpha\delta}{u_*^2}\right)^{\frac{1}{2}}\left(1 - \dfrac{y}{\delta}\right)^2 & \text{for } y_1 < y < \delta. \quad (22d) \end{cases}$$

The coefficients $\mathscr{K}$ and $\mathscr{K}_1$ in these equations are determined by (13) and (15), y_2 is the ordinate of the intersection point of the graphs of the wall law (22*a*, *b*) and 'half-power law' (22*c*), and y_1 is the ordinate of the intersection point of the graphs of the 'half-power law' (22*c*) and 'velocity defect law' (22*d*).

Equations (22) have been used for the computation of all the measured velocity profiles for adverse-pressure-gradient boundary layers from the book by Coles & Hirst (1969) and from the later work by Samuel & Joubert (1974). The values of U_∞, u_*, δ and α used have been taken from the tables in the book by Coles & Hirst and from similar tabulated data of Samuel & Joubert kindly sent to us by Professor A. E. Perry. The ordinates y_2 and y_1 of the intersection points of the half-power law with the wall law and with the velocity defect law have been determined with the aid of a computer. The same computer has also given us the whole profile $U(y)$. If the half-power law (22*c*) does not intersect the velocity defect law (22*d*), then the computer determines the ordinate of the intersection point of the wall law and the velocity defect law and gives the velocity profile $U(y)$ which is obtained with these two laws directly matching each other. We shall see below that such cases produce the worst agreement of the computed velocity profile with the measured one.

We have analysed about 250 different velocity profiles taken from 25 experiments. The results of the calculations appeared to be very satisfactory. As a typical example

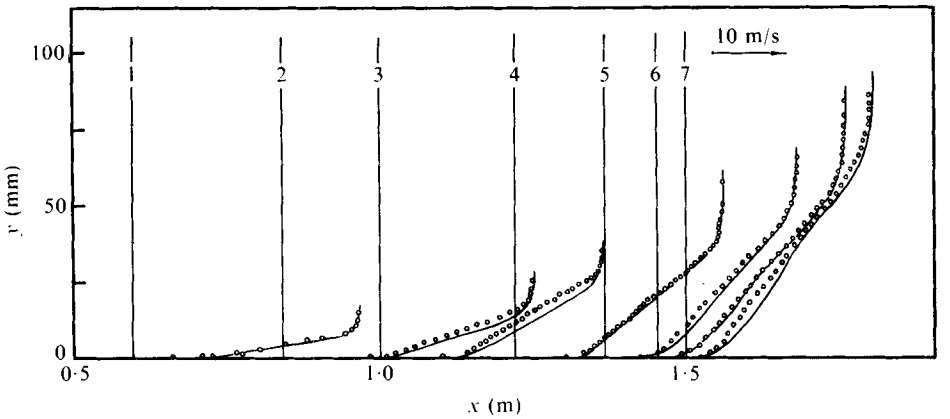

FIGURE 7. Comparison of the velocity profiles measured by Newman (experiment 3500; points) with the proposed theoretical equations (solid lines). The vertical straight lines in this figure and in subsequent similar figures indicate the origins of the velocity values for different profiles. The velocity scale is given in the right upper corner.

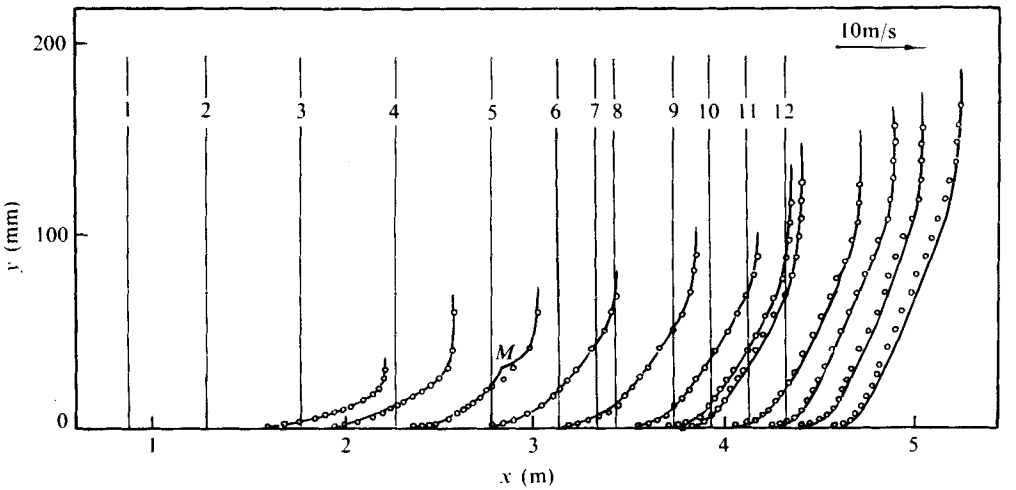

FIGURE 8. Comparison of the velocity profiles measured by Ludwieg & Tillmann (experiment 1100) with the proposed theoretical equations. Notation as in figure 7.

we plot in figure 7 the above-mentioned velocity-profile data of Newman (cf. figure 1 on p. 315) together with the corresponding results of computation with the aid of (22). We see that the deviations of the computations from the measurements do not exceed a few per cent. In figure 8 a similar graph is shown which is related to the Ludwieg & Tillmann (1949) measurements of a boundary layer in a diverging channel (experiment 1100 from Coles & Hirst 1969). The agreement of the computations with the experiment is even better in figure 8 than in figure 7 with the single exception of profile 3. In the case of this profile the half-power law (22*c*) does not intersect the velocity defect law (22*d*) and therefore the computed profile 3 is composed of the wall law (22*b*) and the velocity defect law (22*d*), which join at the point M where a sharp discontinuity in the first derivative appears. At the same time the measured profile 3 is very smooth and includes a considerable portion described by the half-power law,

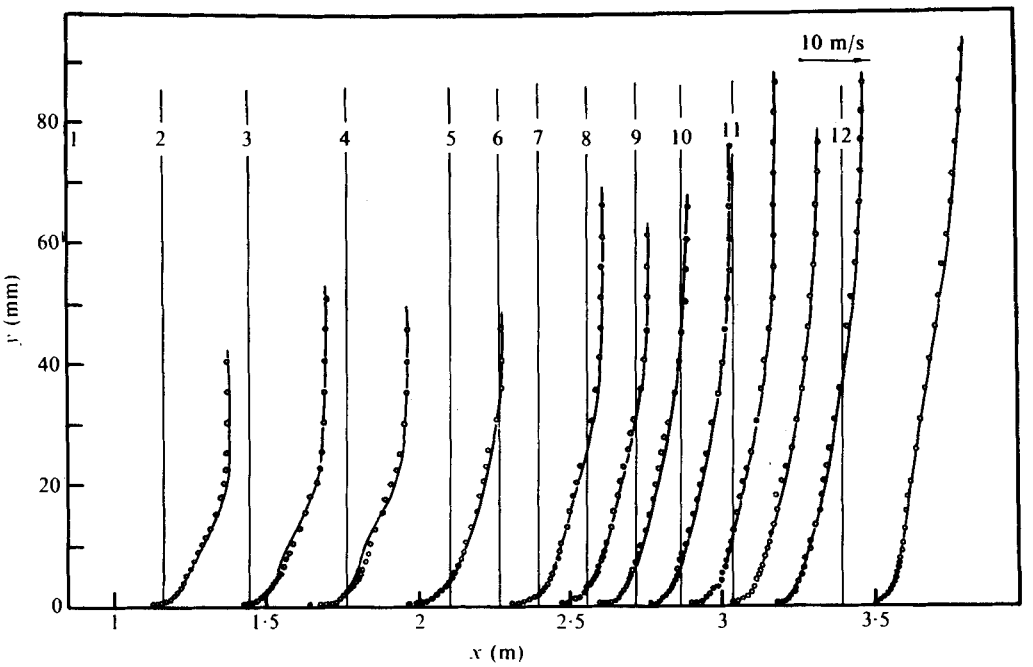

FIGURE 9. Comparison of the velocity profiles measured by Samuel & Joubert (1974) with the proposed theoretical equations. Notation as in figure 7.

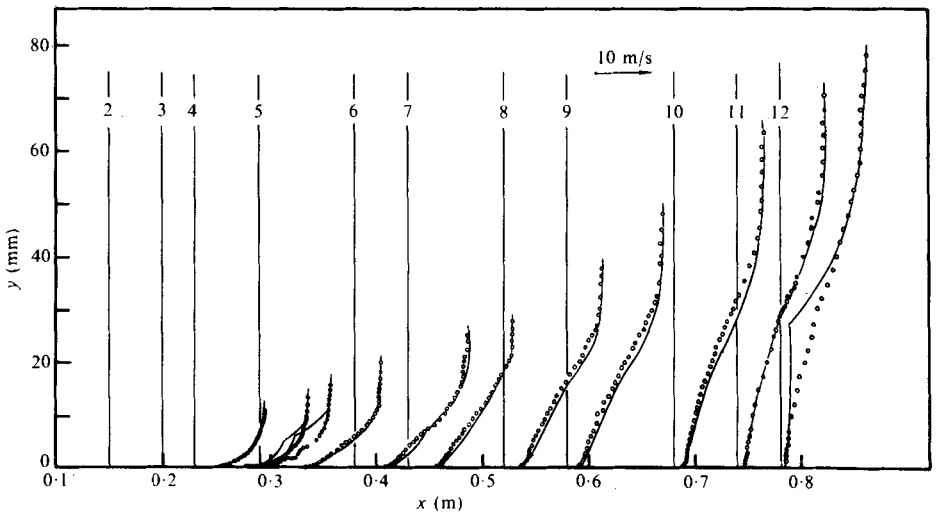

FIGURE 10. Comparison of the velocity profiles measured by Fraser (experiment 5100) with the proposed theoretical equations. Notation as in figure 7.

but with coefficients different from the theoretical recommendations (13) and (15). Nevertheless the relative error in the computed profile is rather small for profile 3 too: it does not exceed 8 %. One more typical example is given in figure 9, where careful experimental data of Samuel & Joubert (1974) are plotted. Finally we want also to show the result of the computation for the experiment yielding the worst agreement

with the data. Thus we have plotted in figure 10 the data of H. R. Fraser (experiment 5100 from Coles & Hirst 1969) related to measurements in a round diffuser for a range of high values of the dimensionless parameter $\alpha\delta/u_*^2$ (extending to $\alpha\delta/u_*^2 = 1440$). This figure shows that among the eleven measured profiles there are three profiles such that the corresponding half-power law (22c) does not intersect the velocity defect law (22d). This leads to the considerable deviation of the computed profiles 3, 4 and, especially, 12 from the measured ones. However, for these profiles too, the relative error is not very great (and is very small for all the other profiles).

Summing up, we may say that for a great variety of adverse-pressure-gradient boundary layers equations (22) describe the measured profiles quite satisfactorily. Significant deviations appear only in a few cases when the half-power law with the coefficients (13) and (15) does not intersect the velocity defect law (22d) while the measured velocity profile includes a considerable interval of y values described by the half-power law but with the coefficients $\mathscr{K}$ and $\mathscr{K}_1$ different from the proposed values. (The deviations of the experimental values of $\mathscr{K}$ and $\mathscr{K}_1$ from the theoretical equations are clearly seen in figures 3 and 4.) The observed discrepancies may be due to the inaccuracy of (13) and (15); moreover it is also possible that the only reason for the discrepancies is the appearance of considerable errors in the measured values u_* and δ. Let us especially note that Fraser's data in figure 10 refer to the flow in very high pressure gradients, where the usual method of the determination of u_* with the aid of the logarithmic approximation to the wall velocity profile is very inaccurate. Moreover Fraser's experiment is related to an axially symmetric, and not plane, flow, while the considerations of the present paper refer mainly to plane flows. Hence we may conclude that there are no reasons at present to modify (13), (15) and (22). We also emphasize that the satisfactory agreement of (22) with the data confirms the assumption of moving equilibrium of most of the boundary layers analysed in Coles & Hirst (1969) and of the boundary layer studied by Samuel & Joubert (1974). Additional remarks on this topic will be given in the part of the next section related to figure 11.

4. The determination of the skin-friction coefficient and the boundary-layer thickness

A family of velocity profiles (22) has been constructed in the previous section and it has been shown that this family agrees well with the data for a wide variety of the boundary layers in adverse pressure gradients. The derived velocity profiles depend on the molecular viscosity ν and on the parameters U_∞, α, δ and u_* at the particular cross-section $x =$ constant. The parameters U_∞ and $\alpha = -U_\infty dU_\infty/dx$ are determined by the free-stream velocity distribution. This distribution is easily measured and therefore it is usually justified to assume that U_∞ and α are known. However, the determination of the friction velocity u_* (or, equivalently, the wall stress $\tau_w = \rho u_*^2$ or skin-friction coefficient $c_f = 2(u_*/U_\infty)^2$) and the boundary-layer thickness δ is a much more difficult task. The present section will be entirely devoted to this determination.

Let us begin with the problem of the determination of u_* (or c_f). Much attention is usually devoted to this problem in the theory of the turbulent boundary layer. It is usually assumed that the following quantities are known: ν, U_∞, some typical boundary-layer thickness Δ (e.g. the usual thickness δ, the displacement thickness δ^*

or the momentum thickness θ) and some integral characteristic of the velocity distribution in the outer region of the boundary layer (e.g. the conventional shape factor $H = \delta^*/\theta$ or some modification of this). The expression for u_* in terms of ν, U_∞, Δ and the velocity distribution characteristic (or, in dimensionless form, the expression for the coefficient c_f in term of the Reynolds number $Re = U_\infty \Delta/\nu$ and some dimensionless shape factor) is called usually a skin-friction law for the boundary layer. Many empirical, semi-empirical or 25 %-empirical forms of the skin-friction law have been proposed by different authors; these laws have different accuracy and different domains of validity (see, for example, Ludwieg & Tillmann 1949; Nash 1966; Mellor & Gibson 1966; Coles & Hirst 1969, pp. 11–14; Kutateladze & Leont'ev 1972). However, none of these skin-friction laws is valid for all the boundary layers analysed in the present paper. Moreover a special form of the skin-friction law is needed in the framework of our theory, namely the form expressing u_* (or c_f) in terms of ν, U_∞, δ and α. Now we shall derive a new form of the skin-friction law applicable to all moving-equilibrium turbulent boundary layers in adverse pressure gradients.

The theoretical derivation of the skin-friction law is usually based on the use of a particular family of velocity profiles. The most traditional derivation uses also the assumption of the existence of an overlap interval in which the wall law and the velocity defect law are valid simultaneously and can be added together (see, for example, the classical paper by Millikan 1939; or the work by Mellor & Gibson 1966, § 3); there are also derivations in which the velocity-profile equation is used differently (e.g. Coles in Coles & Hirst 1969, pp. 11–14). It is important that all the derivations suggest that the wall law has the simplest logarithmic form (3). This leads to the term of the form $A \ln Re$ in the equation for $U_\infty/u_* = (2/c_f)^{\frac{1}{2}}$ which appears in almost all the published boundary-layer skin-friction laws (in particular in the laws of Rotta, Coles, Thompson, Nash and Mellor & Gibson considered in the sources cited above). However, it has already been stressed in the present paper that the logarithmic layer of a flow can be completely destroyed by a pressure gradient when this gradient is strong enough (such a situation arises in all the cases which correspond to the experimental points in figure 4 which deviate significantly from the dashed line). It is clear that usual forms of skin-friction law cannot be applied to boundary layers without a logarithmic layer.

We may use the existence of the generalized half-power layer in all the boundary layers analysed. We have seen that this layer coincides with the overlap layer in which the generalized gradient law (4*a*) [of the special form (11)] and the generalized velocity defect law (7*a*) [of the form (16)] are valid. According to the Millikan method it is sufficient to add (11) and (16) to derive the skin-friction law. Such a procedure leads to the equation

$$\frac{U_\infty}{u_*} = \frac{\mathscr{K}_1}{u_*} + \frac{(\alpha\delta)^{\frac{1}{2}}}{u_*} I\left(\frac{\alpha\delta}{u_*^2}\right), \tag{23}$$

which can be written in the form

$$\frac{U_\infty}{u_*} = 2{\cdot}44 \ln \Gamma - \frac{15}{\Gamma^{\frac{1}{2}}} - \frac{6}{\Gamma} + 10\left[3 + 0{\cdot}16\frac{(\alpha\delta)^2}{u_*^4}\right]^{\frac{1}{4}}, \quad \Gamma = \frac{6u_*^3/\alpha\nu}{50u_*^2/\alpha\delta + 5}, \tag{24}$$

by virtue of (15) and (17). The skin-friction law (24) expresses the quantity

$$U_\infty/u_* = (2/c_f)^{\frac{1}{2}}$$

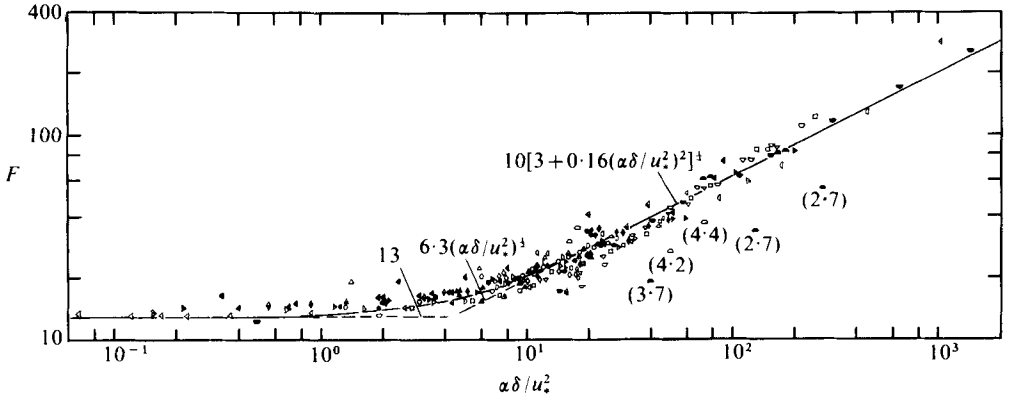

FIGURE 11. The dependence of the parameter F on $\alpha\delta/u_*^2$ for adverse-pressure-gradient boundary layers. The numbers in parentheses below some of the points indicate the values of $U_\infty/(\alpha\delta)^{\frac{1}{2}}$.

in terms of the dimensionless parameters $u_*\delta/\nu$ and $\alpha\delta/u_*^2$. This law permits one to compute the skin-friction coefficient c_f when the values of the Reynolds number $Re = U_\infty\delta/\nu$ and of the modified shape factor $\alpha\delta/U_\infty^2$ are known. (Some details of the corresponding method of computation will be given below.) A comparison of the skin-friction law (24) with the data is shown in figure 11, where the values of the quantity $F = U_\infty/u_* - 2{\cdot}44\ln\Gamma + 15/\Gamma^{\frac{1}{2}} + 6/\Gamma$ are plotted along the y axis and the values of $\alpha\delta/u_*^2$ are plotted along the x axis. The points in figure 11 correspond to the experimental data for all the velocity profiles used in figures 3 and 4 and the solid line is described by the equation $F = 10[3 + 0{\cdot}16(\alpha\delta)^2/u_*^4]^{\frac{1}{4}}$ implied by (24). We see that the points cluster along the theoretical curve with moderate scatter. Moreover most of the points which deviate significantly from the curve correspond to low values of $U_\infty/(\alpha\delta)^{\frac{1}{2}}$ (these values are given in parentheses below some of such points). We mention that it has already been explained in § 2 that the condition for moving equilibrium may not be satisfied accurately enough at low values of $U_\infty/(\alpha\delta)^{\frac{1}{2}}$. Therefore the presence of the significant deviations from the theoretical curve in figure 11 may indicate the low accuracy of the moving-equilibrium condition when applied to some experiments from the book by Coles & Hirst (1969).

It is natural that the data analysed agree with the skin-friction law (24) satisfactorily. In fact, this law is obtained by adding together (11) and (16), and the coefficients of these equations are determined by the treatment of the same data. Let us also stress that the skin-friction law (24) has satisfactory accuracy even in the case $\alpha = 0$ (i.e. for a constant-pressure boundary layer). If $\alpha \to 0$ then $\Gamma \to 3u_*\delta/25\nu \gg 1$. Therefore (24) turns into the equation

$$U_\infty/u_* = 2{\cdot}44\ln(u_*\delta/\nu) + 7{\cdot}8 \tag{25}$$

as $\alpha \to 0$. Equation (25) represents the well-known skin-friction law for a boundary layer in the absence of a longitudinal pressure gradient (see, for example, equation (5.58) in Monin & Yaglom 1971, which differs from (25) only by an insignificant small change in the values of the numerical coefficients). We see that (23) is applicable to all non-negative values of α, beginning from $\alpha = 0$. This is, of course, due to the fact that a narrow region of approximate validity of the generalized half-power law may be found at any non-negative values of α.

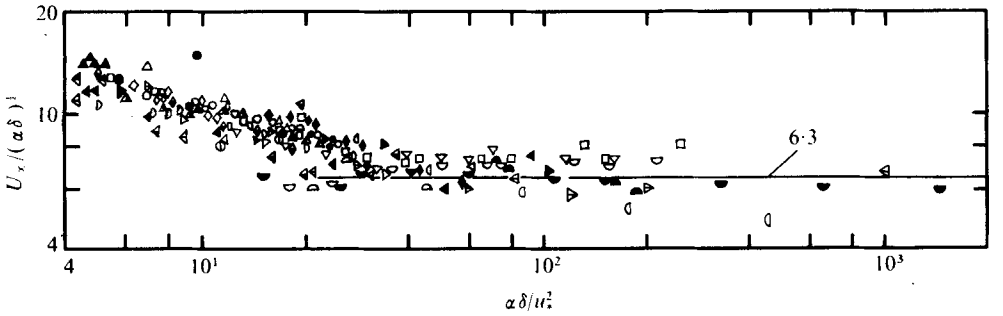

FIGURE 12. The ratio $U_\infty/(\alpha\delta)^{\frac{1}{2}}$ as a function of $\alpha\delta/u_*^2$ for the measured velocity profiles with $\alpha\delta/u_*^2 > 4$.

The situation is more complicated in the extreme case of very high values of $\alpha\delta/u_*^2$ (i.e. large α and small u_*). Formally $\Gamma \to 0$ and $\mathscr{K}_1 \to -\infty$ as $\alpha \to \infty$ and $u_* \to 0$. However, both α and u_* are dimensional quantities and therefore such a passage to the limit is, in fact, unjustified. It is more reasonable to assume that $\alpha\delta/u_*^2 = \delta/\delta_p \to \infty$ but that the value of $r = \delta_p/\delta_v = u_*^3/\alpha\nu$ is fixed; then $\Gamma \to 1{\cdot}2r$ and $\mathscr{K}_1/u_*$ is a definite function of r. The form of this function implied by (15) is, of course, rather unreliable since the equation itself is a crude approximation only. But the exact form of the dependence of $\mathscr{K}_1/u_*$ or r is apparently rather unimportant, since the lower edge of the half-power layer is very near to the wall (in comparison with the distance δ) at large values of $\alpha\delta/u_*^2$. Hence the 'slip velocity' $\mathscr{K}_1$ (representing the velocity of slip at the wall, if the half-power law is extrapolated to the wall) proves to be a very small part of $U_\infty \approx U(\delta)$ in the cases considered. (A very typical example of this is given by Stratford's 1959*b* data.) The arguments above show that the first term on the right-hand side of (23) is usually small in comparison with the left-hand side, if $\alpha\delta/u_*^2 \gg 1$, and hence the first term on the right-hand side may be neglected in the first approximation. Taking into account that $I(\alpha\delta/u_*^2) \approx 6{\cdot}3$ when $\alpha\delta/u_*^2 \gg 1$, we obtain a very simple approximate form of the skin-friction law (23) for strong adverse pressure gradients:

$$U_\infty/(\alpha\delta)^{\frac{1}{2}} \approx \text{constant} \approx 6{\cdot}3 \quad \text{for} \quad \alpha\delta/u_*^2 \gg 1. \tag{26}$$

To verify (26) we plot in figure 12 the values of $U_\infty/(\alpha\delta)^{\frac{1}{2}}$ for all the velocity profiles analysed which are such that $\alpha\delta/u_*^2 > 4$. We see that (26) agrees fairly satisfactorily (namely, with an accuracy of about 15 %) with the data for all the cases for which $\alpha\delta/u_*^2 \geqslant 50$. Hence the validity of (26) is confirmed by experiments. The spread of points in the region $\alpha\delta/u_*^2 \geqslant 50$ of figure 12 may be due to the experimental errors, but it is also possible that it reflects the influence of the upstream history of the flow (i.e. the violation of moving equilibrium) or of the variations in $r = u_*^3/\alpha\nu$ on $U_\infty/(\alpha\delta)^{\frac{1}{2}}$ [cf. the discussion of the scatter in figure 6, which represents the defect law used in the derivation of (26)]. Let us remember in this connexion that $U_\infty/(\alpha\delta)^{\frac{1}{2}}$ determines the order of magnitude of the ratio of the time scale of the longitudinal variation of the free-stream velocity to the time scale of the turbulence in the outer boundary layer (see the closing part of § 2). Since 6·3 is not a very large number, it is possible that the moving-equilibrium condition is not satisfied very accurately within the outer region of boundary layers with high values of $\alpha\delta/u_*^2$ and that this circumstance contributes to the inaccuracy of (26).

Relation (26) may be used for the approximate estimation of the boundary-layer thickness at large values of $\alpha\delta/u_*^2$, but the accuracy of such an estimate will be rather low since the accuracy of (26) is also not high and both sides of (26) must be squared to determine the value of δ. Another approximate method of estimating the boundary-layer thickness which gives more satisfactory results will be described later in the present paper.

Let us note that U_∞ decreases along the x axis in an adverse-pressure-gradient boundary layer while δ increases. Therefore (26) makes us think that in the case of an unseparated turbulent boundary-layer flow the inequality $\alpha\delta/u_*^2 > 50$ can, apparently, be valid over a considerable length in the x direction only if $d\alpha/dx$ is negative there (and rather large in absolute value). Let us also note that (26) clarifies some results of Chawla & Tennekes (1973). These authors suggested writing the velocity defect law in the form $[U_\infty - U(y)]/U_\infty = \Phi(y/\delta)$ when u_* is negligibly small, i.e. $\alpha\delta/u_*^2$ is very large. The use of the velocity scale U_∞ may seem strange since the velocity defect law is usually considered as a law governing the relative motions within the outer part of the boundary layer, i.e. the law may include the differences $U_\infty - U(y)$, but not the value of U_∞ itself. However (26) shows that U_∞ is approximately proportional to $(\alpha\delta)^{\frac{1}{2}}$ for the flows analysed by Chawla & Tennekes. Therefore their form of the velocity defect law is in practice equivalent to the form (7) recommended in the present paper.

Let us now consider the problem of the determination of the boundary-layer thickness δ at different values of x. Several different equations describing the dependence of the typical boundary-layer thickness Δ on x can be found in the literature (see, for example, Bam-Zelikovich 1954; Rotta 1962; or Hudimoto 1965). However most of these equations refer to a thickness Δ different from δ (i.e. to the displacement thickness δ^* or the momentum thickness θ) and have an insufficiently wide domain of applicability. A very simple and sufficiently accurate approximate method of determination of the function $\delta(x)$ was proposed for the case $\alpha = 0$ by Landau & Lifshitz (1963, § 44; see also Monin & Yaglom 1971, § 5.6). Their derivation is based on the assumption that the rate v of increase of the boundary-layer thickness is proportional to the typical value of the vertical velocity fluctuation at $y = \delta$. This assumption may be justified by dimensional reasoning. In fact, both the rate v and the scale v' of the vertical velocity fluctuations at $y = \delta$ are evidently determined by turbulence conditions within the outer region of the boundary layer. Hence, if the scale v' is determined by dimensional analysis to within a numerical factor, then the rate v must be proportional to v'. If $\alpha = 0$, then the outer-region turbulence depends on the two dimensional parameters u_* and δ; therefore both v and v' must be proportional to u_*. In other words the equation $d\delta/dt = b_1 u_*$ must be valid in a coordinate system moving with the free-stream velocity U_∞, where b_1 is a numerical constant of the order of unity. (The constant b_1 must, of course, be the same for smooth- and rough-wall flows and also for flows of pure liquids and turbulent flows of solutions of drag-reducing polymers.) This means that

$$\frac{d\delta}{dx} = b_1 \frac{u_*}{U_\infty}, \quad \delta(x) = \delta(x_0) + b_1 \int_{x_0}^{x} \frac{u_*}{U_\infty}\, dx. \tag{27}$$

Let us also note that U_∞ is independent of x when $\alpha = 0$ and u_* varies only very slowly with x (approximately as $x^{-\frac{1}{14}}$; cf. Monin & Yaglom 1971, equation 5.66).

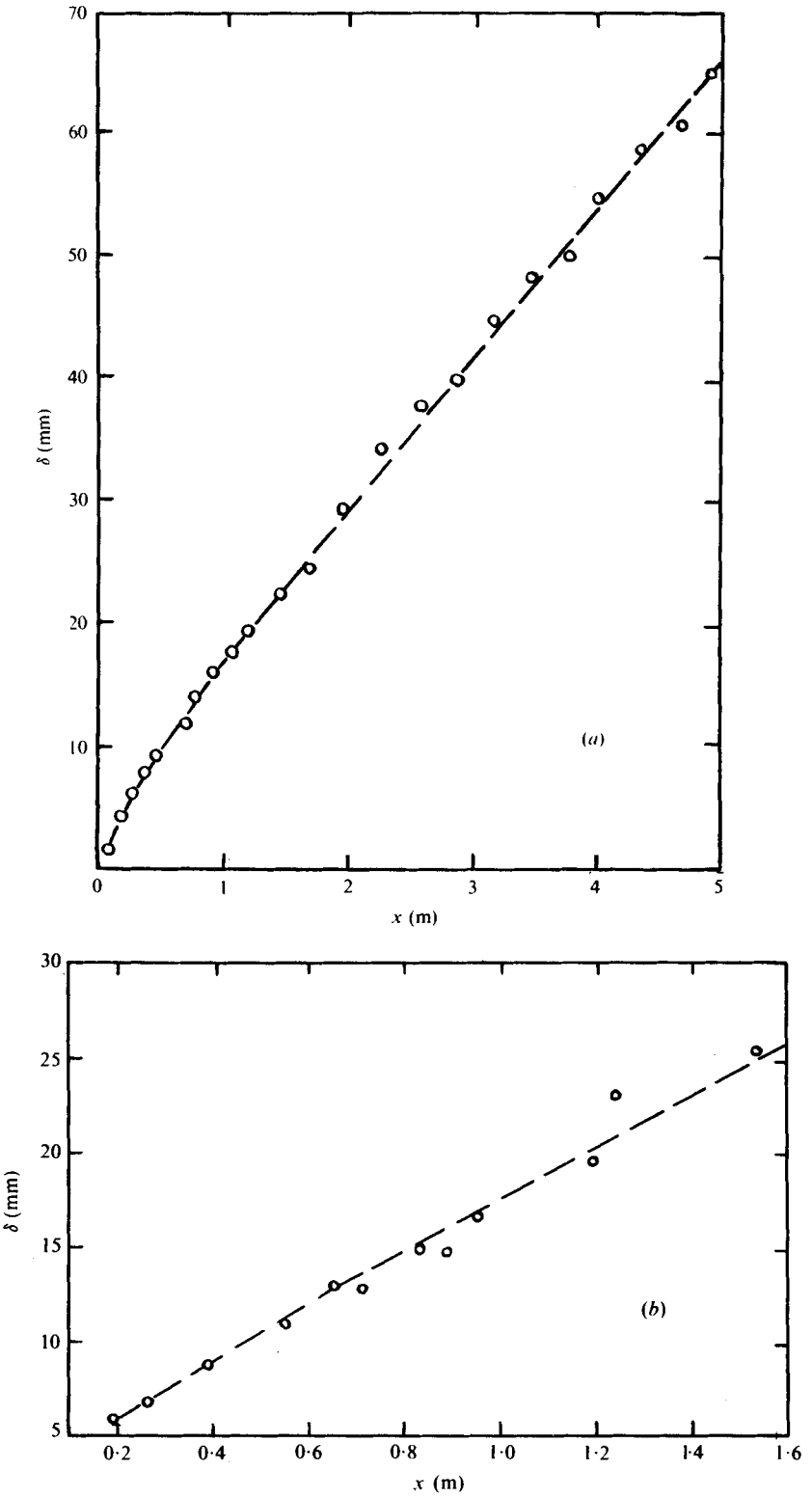

FIGURE 13. The dependence of the boundary-layer thickness of a constant-pressure turbulent boundary layer on the streamwise co-ordinate x. (*a*) Wieghardt's data (experiment 1400). (*b*) Bell's data (experiment 3000). The dashed lines correspond to (28) with $b = 0{\cdot}34$.

Therefore the second of equations (27) may be replaced by the simpler approximate equation

$$\delta(x) = \delta(x_0) + b(u_*/U_\infty)(x - x_0), \tag{28}$$

where the numerical coefficient b differs from b_1 only slightly (and therefore these two coefficients must be considered as equal when we are not demanding high accuracy). To determine the value of the coefficient b we compare (28) with the data of Wieghardt and Bell for constant-pressure boundary layers from the book by Coles & Hirst (see figures 13*a*, *b*). We see that both the experiments confirm the validity of (28) and imply the same value $b = 0{\cdot}34$ of the coefficient.

The general case of a boundary layer with a pressure gradient (with an arbitrary value of α) was considered by Hudimuto (1965). This author also assumed that $d\delta/dx$ is proportional to v'/U_∞ where v' is the scale of vertical velocity fluctuations at $y = \delta$. However he determined v' with the aid of a special semi-empirical hypothesis and an assumption concerning the form of the velocity profile $U(y)$. In this paper we shall use the assumption that $d\delta/dx \propto v'/U_\infty$ but we shall determine v' with the aid of dimensional reasoning. Let us begin with the limiting case $\alpha\delta/u_*^2 \gg 1$. In this case the turbulence conditions in the outer part of the boundary layer are influenced by the parameters α and δ. Hence both the velocity scales v' and v must be proportional to $(\alpha\delta)^{\frac{1}{2}}$, i.e.

$$d\delta/dx = a_1(\alpha\delta)^{\frac{1}{2}}/U_\infty, \tag{29}$$

where a_1 is another numerical coefficient of the order of unity.† Let us now remember that the skin-friction law (24) implies the approximate equation (26) when $\alpha\delta/u_*^2 \gg 1$ and that the data from Coles & Hirst (1969) also confirm the approximate validity of this equation. (It is easy to see that (26) can be compatible with (29) only if $d\alpha/dx$ is negative and not too small in absolute value. This fact is however of no importance here.) Therefore (29) may also be rewritten in the following form:

$$d\delta/dx \approx c_1 = \text{constant}, \quad c_1 \approx a_1/6{\cdot}3, \quad \text{when} \quad \alpha\delta/u_*^2 \gg 1. \tag{30}$$

This equation shows that the boundary-layer thickness must increase approximately linearly with x (and that the rate of increase must be almost constant) when $\alpha\delta/u_*^2 \gg 1$ (apparently when $\alpha\delta/u_*^2 > 50$). The verification of the last result is considerably complicated by the fact that the condition $\alpha\delta/u_*^2 > 50$ is usually valid for a small portion of the x axis only, after which separation appears. Moreover the moving-equilibrium condition is not usually satisfied accurately enough for boundary layers close to the separation. Nevertheless it is possible to compare the prediction (30) with the data of ten experiments from Coles & Hirst (1969) which include velocity-profile measurements at several adjusting stations satisfying the condition $\alpha\delta/u_*^2 > 50$. In

† We note that for the case of a turbulent boundary layer in a strong adverse pressure gradient the equation $d\delta/dx \approx a\alpha\delta/U_\infty^2$ was suggested by Bam-Zelikovich (1954). By virtue of (26) this equation differs from (29) only slightly. However Bam-Zelikovich assumed that any typical boundary-layer thickness may be used as δ and compared his equation with data for the case when δ was a displacement thickness or a momentum thickness. On the basis of the entrainment method of boundary-layer theory (see, for example, Head in Kline *et al.* 1969, pp. 188–194) and the relative smallness of δ^* compared with δ, one may try replacing the right-hand side of (29) by $U_\infty^{-1} d(U_\infty \delta)/dx$. (Such a replacement changes nothing when $\alpha = 0$ and $U_\infty = \text{constant}$, but it does lead to a change when $\alpha \neq 0$.) However it appears that such a change does not give better agreement with the data.

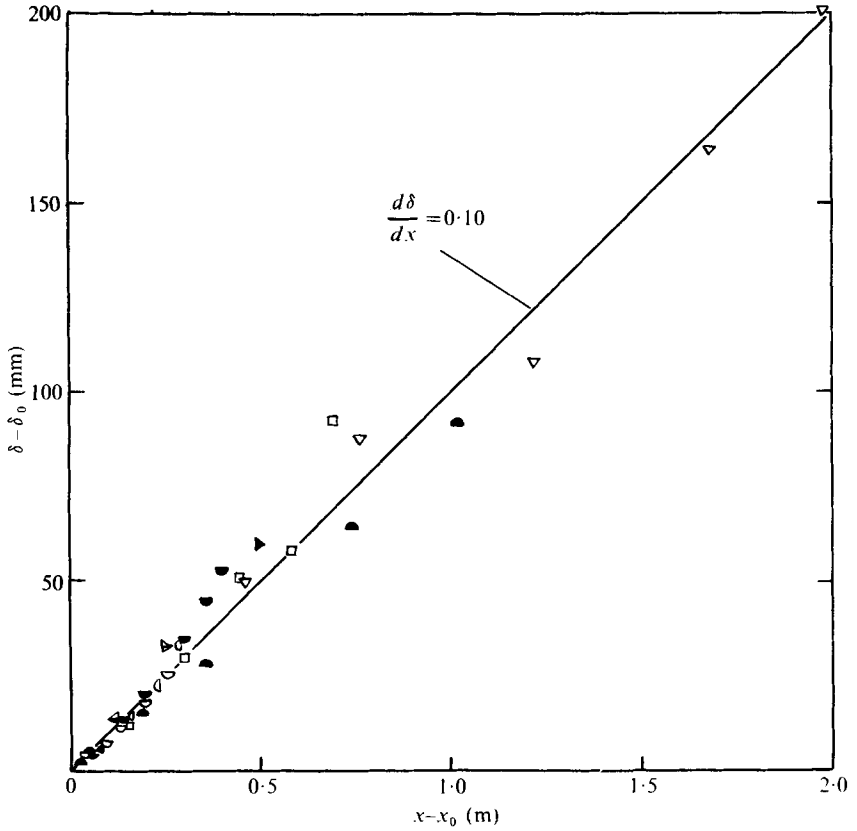

FIGURE 14. The dependence of the increase in the boundary-layer thickness on the increase in the streamwise co-ordinate for strongly decelerated turbulent boundary layers with $\alpha\delta/u_*^2 > 50$.

figure 14 we plot $\delta - \delta_0$, where $\delta_0 = \delta(x_0)$, as a function of $x - x_0$ for all these measurements related to unseparated flows; here x_0 is the x co-ordinate of the first of the indicated station points. There is a considerable spread of points in figure 14 but all the points nevertheless clearly cluster around the line $\delta - \delta_0 = 0{\cdot}1(x - x_0)$. We may therefore consider figure 14 as a confirmation of the theoretical prediction (30) and deduce from it that $c_1 \approx 0{\cdot}1$, i.e. $a_1 \approx 0{\cdot}63$.

The dimensional analysis does not permit one to determine uniquely the rate of increase of $\delta(x)$ with x at intermediate (not too small and not too great) values of $\alpha\delta/u_*^2$. In this case the dimensional analysis implies only that $v = u_* \psi(\alpha\delta/u_*^2)$, i.e.

$$\frac{d\delta}{dx} = \frac{u_*}{U_\infty} \psi\left(\frac{\alpha\delta}{u_*^2}\right), \tag{31}$$

where $\psi(s)$ is an unknown function of one variable. By virtue of (27) and (29) this function must have the following asymptotics: $\psi(s) \to b_1 \approx 0{\cdot}34$ when $s \to 0$ and $\psi(s) \approx a_1 s^{\frac{1}{2}}$, $a_1 \approx 0{\cdot}63$, when $s \gg 1$. This makes it possible to try to choose the approximate form of $\psi(s)$ by means of interpolation between two asymptotics. However the interpolation equations of the form used above to find the variation of the functions $\mathscr{K}(\alpha\delta/u_*^2)$ and $\Phi_3(\eta, \alpha\delta/u_*^2)$ with the argument $\alpha\delta/u_*^2$ do not give good agreement

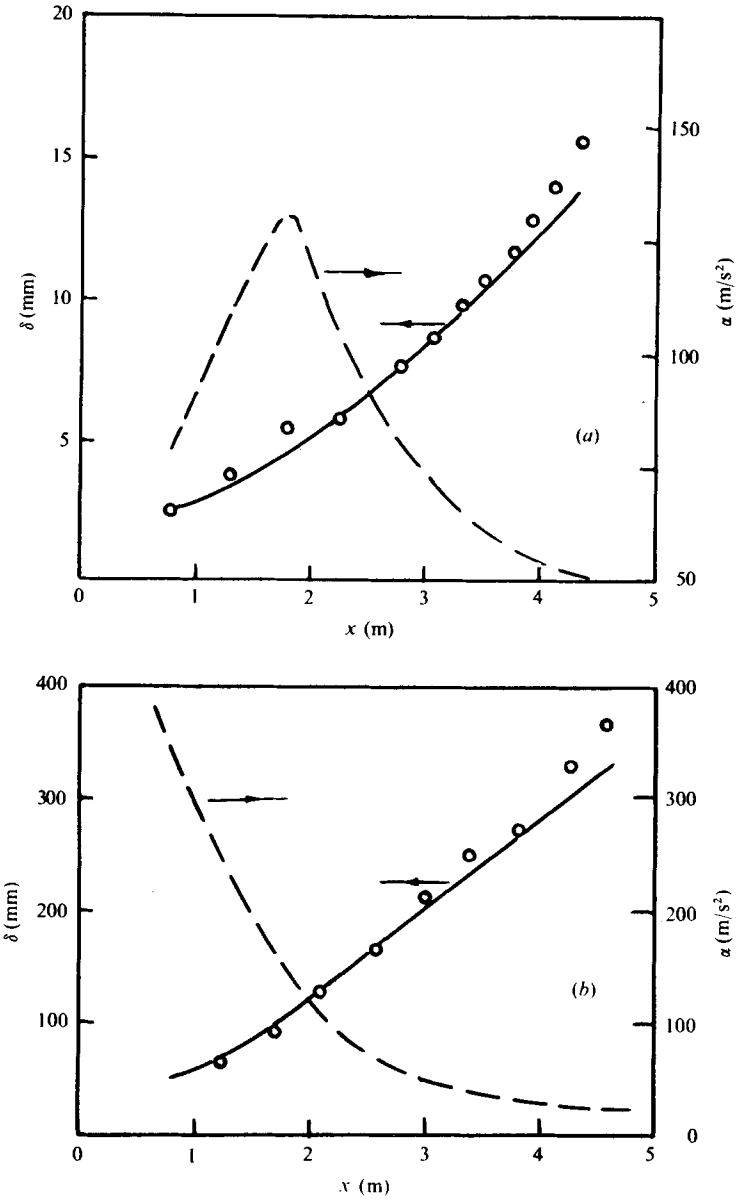

FIGURE 15. Comparison of the measured dependence of the boundary-layer thickness on x (points) with the computation according to (33) (solid lines). The dashed lines indicate the corresponding dependence of α on x. (*a*) Ludwieg & Tillmann's data (experiment 1100). (*b*) Perry's data (experiment 2900).

with the data when applied to $\psi(s)$.† Better agreement may be achieved by use of a combined ('two-layer') interpolation equation. We shall thus use the following combined equation for $\psi(s)$:

$$\psi(s) = \begin{cases} 0{\cdot}34 + 0{\cdot}0824s & \text{when} \quad s < 50, \\ 0{\cdot}63s^{\frac{1}{2}} & \text{when} \quad s > 50. \end{cases} \tag{32}$$

It is easy to see that the function (32) is continuous. It leads to the differential equation

$$\frac{d\delta}{dx} = \begin{cases} (0{\cdot}34 + 0{\cdot}0824\alpha\delta/u_*^2)\, u_*/U_\infty & \text{when} \quad \alpha\delta/u_*^2 < 50, \\ 0{\cdot}63(\alpha\delta)^{\frac{1}{2}}/U_\infty & \text{when} \quad \alpha\delta/u_*^2 > 50 \end{cases} \tag{33}$$

for the function $\delta(x)$. The results of numerical integration of this equation with the values of $\delta(0)$ and $u_*(x)$ corresponding to experiments 1100 and 2900 from the book by Coles & Hirst (1969) are compared in figure 15 with the results of the direct measurements of $\delta(x)$. We see that the calculated and measured data for $\delta(x)$ are very close to each other. All the other experiments analysed in the present paper provide approximately the same agreement of the theory with the data.

Let us now note that the skin-friction law (24) and boundary-layer-thickness equation (33) permit one to calculate the velocity profiles (22) in cases when only the free-stream velocity distribution $U_\infty(x)$ [and thus $\alpha(x)$] and the boundary-layer thickness $\delta(x_0)$ at the first measurement station are known from experiment. In fact the value of $u_*(x_0)$ can be determined from the values of $U_\infty(x_0)$, $\alpha(x_0)$ and $\delta(x_0)$with the aid of (24).‡ Then we may determine the value of $\delta(x_1)$ at the next point $x_1 = x_0 + \Delta x$ by means of (33). Now we know the values of U_∞, α and δ at $x = x_1$ and therefore we may determine $u_*(x_1)$ with the aid of (24) etc.|| When all the values $U_\infty(x)$, $\alpha(x)$, $\delta(x)$ and $u_*(x)$ are known it is easy to compute the velocity profile $U(y)$ of (22) for every value of x. We have done such a complete profile computation for all the profiles mentioned at the end of § 3. (A more elementary computation of the velocity profile (22) has been described in § 3. This computation is based on the experimental values of the quantities $u_*(x)$ and $\delta(x)$.) The new computed results appear to be rather close to the results of the computation in § 3 and the agreement of the new results with the data is almost as good as that for the old ones. We shall consider here only experiment 1100 of Ludwieg & Tillmann, which is very typical. The comparison of the measured values of $\delta(x)$ for this experiment with the new computation of $\delta(x)$ is shown in figure 16; this figure differs from figure 15(*a*) by the fact that the values of $u_*(x)$ in the

† Quite satisfactory agreement can be obtained if some more complicated interpolation equation is used. For example, the function $\psi(s) = [5 + (1 + 10/s)^{\frac{3}{2}}]s^{\frac{1}{2}}/10(1 + 10/s)$ gives results which are very close to those implied by (32), but this equation seems to be simpler than the indicated form of $\psi(s)$.

‡ To determine u_* it is convenient at first to express all the terms of (24) as functions of the dimensionless combinations $Re = U_\infty \delta/\nu$, $G = \alpha\delta/U_\infty^2$ and $\lambda = u_*/U_\infty = (2/c_f)^{\frac{1}{2}}$. Then we can pass to the computer determination of the minimum squared difference between the left-hand and right-hand sides of (24) considered as functions of one variable λ dependent on parameters Re and G. It is reasonable to begin the search for the minimum at the point $x = x_0$, assuming that $\lambda = \lambda_0$, where λ_0 is the value of λ for a constant-pressure boundary layer at the same value of Re. It is also convenient to begin the search for the minimum at the subsequent points $x = x_i$ assuming that $\lambda = \lambda_{i-1}$, where $\lambda_{i-1} = \lambda(x_{i-1})$ is the value of λ corresponding to the latest calculation.

|| The solution of the system of equations (33) and (24) may be performed by a method of successive approximation (only a few approximations are in fact needed in practice).

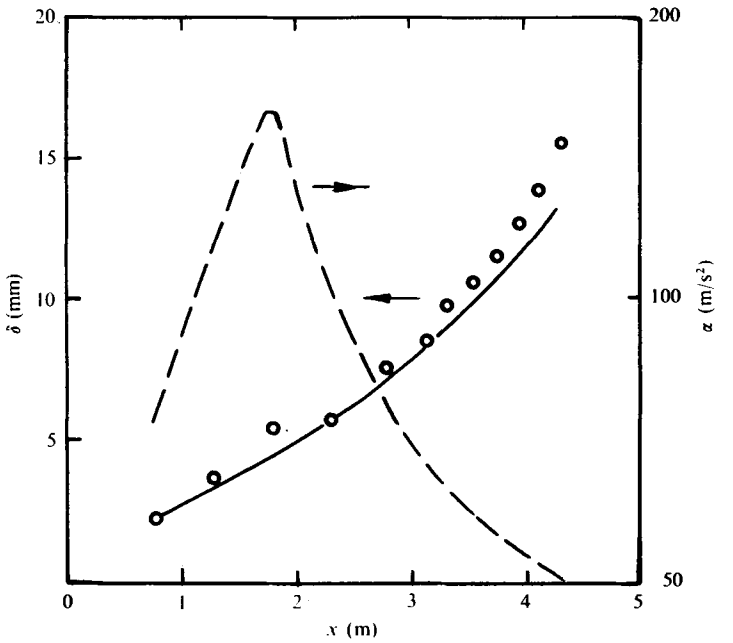

FIGURE 16. The comparison of the dependence of the boundary-layer thickness δ on x measured by Ludwieg & Tillmann with the computation according to equation (33) where the values of u_* are determined for every x with the aid of skin-friction law (24).

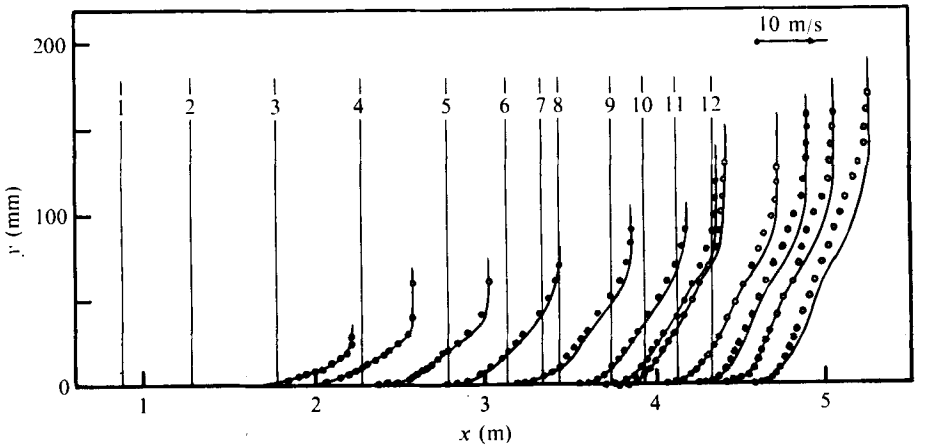

FIGURE 17. The comparison of the velocity profiles measured by Ludwieg & Tillmann with the equations (22) where the values of u_* and δ are calculated with the aid of the proposed theoretical equations.

left-hand side of (33) are now determined with the aid of (24). We see that new computed values of $\delta(x)$ differ slightly from the computed values in figure 15(a). The new computation of the velocity profiles $U(y)$ for all the measurement stations of experiment 1100 is shown in figure 17. We see that the new computed velocity profiles agree with the data approximately as well as the results of the computation in figure 8, where it is supposed that the values of $U_\infty(x)$, $\alpha(x)$, $\delta(x)$ and $u_*(x)$ are all known

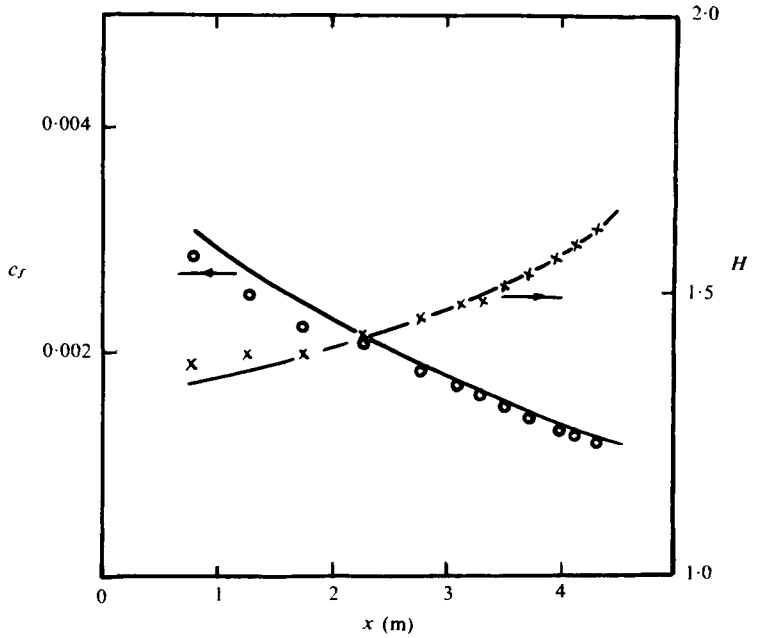

FIGURE 18. The comparison of the computed values of the skin-friction coefficient c_f and of the shape factor H (lines) with the corresponding experimental values of Ludwieg & Tillmann (points).

from the experiment. (We mention that the new profile 3 agrees with the data excellently in contrast to profile 3 in figure 8. However the new computed profiles 9–12 agree less well with the data than the same profiles in figure 8; this is apparently due to the underestimation of the δ values for the corresponding measurement stations which is observed in figure 16.) Finally, a comparison of the computed values of the skin-friction coefficient c_f and of the shape factor $H = \delta^*/\theta$ with the corresponding experimental values (determined from the measured velocity profiles) is shown in figure 18. The agreement of the theory with the data is quite good in this case too. Therefore we may conclude that the proposed method of velocity-profile computation for adverse-pressure-gradient boundary layers leads to very satisfactory results also in the case when only the function $U_\infty(x)$ and the value of δ at the first measurement station are known from experiment.

The authors are grateful to Professor A. E. Perry, who sent them a copy of the report by Schofield & Perry (1972) and the tabulated experimental data of Samuel & Joubert (1974). They also thank Professor D. Coles, who kindly provided them with copies of both volumes of the *Proceedings of the* 1968 *AFOSR–IFP Stanford Conference*. Finally they want to thank Professor R. L. Simpson, who sent them the numerical data of very careful recent measurements by Simpson, Strickland & Barr (1977) .These data were received when the present paper had been already finished and sent to the publishers, therefore they were not used in the text above. However the authors have now finished the treatment of the data and are glad to note here that all the measurements by Simpson *et al.* related to an adverse-pressure-gradient unseparated boundary layer prove to agree excellently with the above equations.

REFERENCES

ALLAN, W. K. & SHARMA, V. 1974 An investigation of two turbulent flows over smooth and rough surfaces. *J. Mech. Engng Sci.* **16**, 71–78.

BADRI NARAYANAN, M. A. & RAMJEE, V. 1969 On the criteria for reverse transition in a two-dimensional boundary layer flow. *J. Fluid Mech.* **35**, 225–241.

BAM-ZELIKOVICH, G. M. 1954 Computation of the boundary layer separation. *Izv. Akad. Nauk SSSR, Otdel. Tekh. Nauk* (*Bull. Acad. Sci. USSR, Div. Engng Sci.*), no. 12, pp. 68–85.

BARENBLATT, G. I. 1976 Self-preservation: similarity and intermediate asymptotics. *Izv. Vysch. Uchebn. Zaved. SSSR, Radiofiz.* (*Proc. Univ. Coll. USSR, Ser. Radiophys.*) **19**, 902–931.

BARENBLATT, G. I. & ZEL'DOVICH, YA. B. 1972 Self-similar solutions as intermediate asymptotics. *Ann. Rev. Fluid Mech.* **4**, 285–312.

BRADSHAW, P. 1969 A note on reverse transition. *J. Fluid Mech.* **35**, 387–390.

BRIDGMAN, P. W. 1932 *Dimensional Analysis.* Yale University Press.

BUSINGER, J. A., WYNGAARD, J. C., IZUMI, Y. & BRADLEY, E. F. 1971 Flux-gradient relationships in the atmospheric surface layer. *J. Atmos. Sci.* **28**, 181–189.

CEBECI, T. & SMITH, A. M. O. 1974 *Analysis of Turbulent Boundary Layers.* Academic Press.

CHAWLA, T. C. & TENNEKES, H. 1973 Turbulent boundary layers with negligible wall stress: a singular-perturbation theory. *Int. J. Engng Sci.* **11**, 45–64.

CLAUSER, F. H. 1956 The turbulent boundary layer. *Adv. Appl. Mech.* **4**, 1–51.

COLES, D. & HIRST, E. 1969 *Comp. Turbulent Boundary Layers. Proc.* 1968 *AFOSR–IFP Stanford Conf.* vol. 2. *Data Compilation.*

ENGELUND, F. 1973 Analogy between the velocity distribution in a stable atmosphere and in divergent channels. *Phys. Fluids* **16**, 1768–1770.

FEDYAEVSKII, K. K., GINEVSKII, A. S. & KOLESNIKOV, A. V. 1973 *Computation of the Turbulent Boundary Layer of Incompressible Fluid.* Leningrad: Publ. House 'Sudostroenie'.

GINEVSKII, A. S. 1969 *Theory of the Turbulent Jets and Wakes.* Moscow: Publ. House 'Mashinostroenie'.

GINEVSKII, A. S. & SOLODKIN, E. E. 1958 Transverse wall curvature effects on the characteristics of an axially symmetric turbulent boundary layer. *Prikl. Mat. Mekh.* (*Appl. Math. Mech.*) **22**, 819–825.

HEAD, M. R. 1976 Equilibrium and near-equilibrium turbulent boundary layers. *J. Fluid Mech.* **73**, 1–8.

HINZE, J. O. 1975 *Turbulence*, 2nd edn. McGraw-Hill.

HUANG, T. T. 1974 Similarity laws for turbulent flow of dilute solutions of drag-reducing polymers. *Phys. Fluids* **17**, 298–309.

HUDIMOTO, B. 1965 A method for the calculations of the turbulent boundary layer with pressure gradient. *Kyoto Univ. Faculty Engng Memoirs* **27**, 433–442.

IZAKSON, A. A. 1937 On the formula for the velocity distribution near walls. *Tech. Phys. USSR* **4**, 155–162.

KADER, B. A. & YAGLOM, A. M. 1972 Heat and mass transfer laws for fully turbulent wall flows. *Int. J. Heat Mass Transfer*, **15**, 2329–2351.

KADER, B. A. & YAGLOM, A. M. 1977*a* Turbulent heat and mass transfer from a wall with parallel roughness ridges. *Int. J. Heat Mass Transfer* **20**, 345–357.

KADER, B. A. & YAGLOM, A. M. 1977*b* Application of the similarity considerations to the computation of decelerated turbulent boundary layers. *Dokl. Akad. Nauk SSSR* **233**, 52–55.

KLINE, S. J., MORKOVIN, M. V., SOVRAN, G. & COCKRELL, D. J. 1969 *Comp. Turbulent Boundary Layers. Proc.* 1968 *AFOSR–IFP Stanford Conf.* vol. 1. *Methods, Predictions, Evaluation and Flow Structure.*

KRESKOVSKY, J. P., SHAMROTH, S. J. & MCDONALD, H. 1975 Application of a general boundary layer analysis to turbulent boundary layers subjected to strong favorable pressure gradients. *Trans. A.S.M.E., J. Fluid Engng* **97**, 217–224.

KUTATELADZE, S. S. & LEONT'EV, A. I. 1972 *Heat Mass Transfer and Friction in a Turbulent Boundary Layer.* Moscow: Publ. House 'Energiya'.

LANDAU, L. D. & LIFSHITZ, E. M. 1963 *Fluid Mechanics*. Pergamon.

LAPIN, YU. V. & SHAROV, V. G. 1974 Turbulent boundary layer of the incompressible fluid in large longitudinal pressure gradients and in the presence of injection. *Izv. Akad. Nauk SSSR, Ser. Mekh. Zh. i Gaza* (*Bull. Acad. Sci. USSR, Ser. Mech. Liquid & Gas*), no. 2, pp. 23–29.

LUDWIEG, H. & TILLMANN, W. 1949 Untersuchungen über die Wandschubspannung in turbulenten Reibungsschichten. *Ing.-Arch.* **17**, 288–299.

MCDONALD, H. 1969 The effect of pressure gradient on the law of the wall in turbulent flow. *J. Fluid Mech.* **35**, 311–336.

MELLOR, G. L. 1966 The effects of pressure gradients on turbulent flow near a smooth wall. *J. Fluid Mech.* **24**, 255–274.

MELLOR, G. L. & GIBSON, D. M. 1966 Equilibrium turbulent boundary layers. *J. Fluid Mech.* **24**, 225–253.

MILLIKAN, C. B. 1939 A critical discussion of turbulent flows in channels and circular tubes. *Proc. 5th Int. Cong. Appl. Mech., Cambridge, Mass.*, pp. 386–392.

MONIN, A. S. & YAGLOM, A. M. 1971 *Statistical Fluid Mechanics*, vol. 1. MIT Press.

NASH, J. F. 1966 A note on skin-friction laws for the incompressible turbulent boundary layers. *Aero. Res. Counc. Current Paper* no. 862.

NEWMAN, B. G. 1951 Some contributions to the study of the turbulent boundary layer near separation. *Austr. Dept. Supply Rep.* ACA-53.

NG, K. H. & SPALDING, D. B. 1976 Predictions of two-dimensional boundary layers on smooth walls with a two-equation model of turbulence. *Int. J. Heat Mass Transfer* **19**, 1161–1172.

NOVOZHILOV, V. V. 1976 One-layer theory of steady turbulent incompressible flows and its application to the computation of equilibrium turbulent boundary layers. *Vestnik L.G.U.* (*Leningrad State Univ. Herald*), no. 13, pp. 129–145.

PATEL, V. C. & HEAD, M. R. 1968 Reversion of turbulent to laminar flow. *J. Fluid Mech.* **34**, 371–392.

PERRY, A. E. 1966 Turbulent boundary layers in decreasing adverse pressure gradients. *J. Fluid Mech.* **26**, 481–506.

PERRY, A. E., BELL, J. B. & JOUBERT, P. N. 1966 Velocity and temperature profiles in adverse pressure gradient turbulent boundary layers. *J. Fluid Mech.* **25**, 299–320.

PERRY, A. E. & SCHOFIELD, W. H. 1973 Mean velocity and shear stress distributions in turbulent boundary layers. *Phys. Fluids* **16**, 2068–2074.

REEVES, B. L. 1974 Two-layer model of turbulent boundary layers. *A.I.A.A. J.* **12**, 932–939.

ROTTA, J. C. 1962 Turbulent boundary layers in incompressible flow. *Prog. Aero. Sci.* **2**, 1–219.

SAMUEL, A. E. & JOUBERT, P. N. 1974 A boundary layer developing in an increasingly adverse pressure gradient. *J. Fluid Mech.* **66**, 481–505.

SANDBORN, V. A. & KLINE, S. J. 1961 Flow models in boundary layer stall inception. *Trans. A.S.M.E., J. Basic Engng* **83**, 317–327.

SCHOFIELD, W. H. & PERRY, A. E. 1972 The turbulent boundary layer as a wall confined wake. *Austr. Dept. Supply, Aero. Res. Lab, Mech. Engng Rep.* no. 134.

SCHRAUB, F. A. & KLINE, S. J. 1965 A study of the structure of the turbulent boundary layers with and without longitudinal pressure gradients. *Thermosci. Div., Dept. Mech. Engng, Stanford Univ. Rep.* MD-12.

SIMPSON, R. L., STRICKLAND, J. H. & BARR, P. W. 1977 Features of a separating turbulent boundary layer in the vicinity of separation. *J. Fluid Mech.* **79**, 553–594.

STRATFORD, B. S. 1959*a* The prediction of separation of the turbulent boundary layer. *J. Fluid Mech.* **5**, 1–16.

STRATFORD, B. S. 1959*b* An experimental flow with zero skin-friction throughout its region of pressure rise. *J. Fluid Mech.* **5**, 17–35.

TENNEKES, H. 1968 Outline of a second-order theory of turbulent pipe flow. *A.I.A.A. J.* **6**, 1735–1740.

TENNEKES, H. & LUMLEY, J. L. 1972 *A First Course in Turbulence*. MIT Press.

TOWNSEND, A. A. 1960 The development of boundary layers with negligible wall stress. *J. Fluid Mech.* **8**, 143–155.

TOWNSEND, A. A. 1961 Equilibrium layers and wall turbulence. *J. Fluid Mech.* **11**, 97–120.

TOWNSEND, A. A. 1965 Self-preserving flow inside a turbulent boundary layer. *J. Fluid Mech.* **22**, 773–797.

TOWNSEND, A. A. 1976 *The Structure of Turbulent Shear Flow*, 2nd edn. Cambridge University Press.

YAGLOM, A. M. & KADER, B. A. 1974 Heat and mass transfer between a rough wall and turbulent fluid flow at high Reynolds and Péclet numbers. *J. Fluid Mech.* **62**, 601–623.